Kirk-Othmer Encyclopedia of Chemical Technology.

INFORMATION STORAGE MATERIALS, OPTICAL

A most important element in computer technology is data storage. Progress in microelectronics, therefore, is directly linked to progress in data storage, that is the ability to store large amounts of information in the smallest possible space, irreversibly or preferably reversibly.

For data storage two types of memory are distinguished: (*1*) main memory with moderate capacity (currently 4×10^6 bit in each element) and extremely short access time ($\leq 10^{-7}$ s), and (*2*) mass memory with very high capacity ($\geq 10^7$ bit in each element) and moderate access time ($\geq 10^{-2}$ s).

Main memories almost exclusively consist of semiconductors on a silicon basis in complementary metal oxide semiconductor technology (CMOS). The most important types are the pure read only memory (ROM) and the write/read memory (RAM = random access memory), which is available as S-RAM (static RAM) or as D-RAM (dynamic RAM).

The most important mass memories use magnetic media in the form of magnetic tapes or disks (floppy disk and hard disk). Laser addressed optical mass memories are of increasing commercial importance.

Polymers are only marginally important in main memories of semiconductor technology, except for polymeric resist films used for chip production. For optical mass memories, however, they are important or even indispensable, being used as substrate material (in WORM, EOD) or for both substrate material and the memory layer (in CD-ROM). Peripheral uses of polymers in the manufacturing process of optical storage media are, eg, as binder for dye-in-polymer layers or as surfacing layers, protective overcoatings, uv-resist films, photopolymerization lacquers for replication, etc.

Photopolymers and photothermoplasts are mentioned only in connection with holographic data storage (see Holography). The classical method of optical data storage in silver halide films (photographic film, microfiche technique) is not discussed (see Photography).

1. Classification

In general, the commercially used optical data storage media deposit the information on disks or cards (two-dimensional data deposition, Table 1). Data storage systems, which store data in three and more dimensions are being developed.

Depending on the method of data read-out, respectively read-in/read-out, two systems are distinguished: mechanooptical systems with usually disk-shaped media (optical disks), and purely optical systems with card-shaped media without moving parts (optical memory cards).

The disk-shaped optical data storage media can be differentiated into three classes: (*1*) CD-ROM (compact disk-read only memory) in which data are embossed by the manufacturer. The lay-out of the disks and information storage are analogous to the well-known audio compact disk. (*2*) In WORM (write once, read many times), data are written by the user, but are not erasable or rewritable. (*3*) In EOD (erasable optical disk), data are written by the user and can be erased or overwritten. EOD was formerly known as E-DRAW (erasable-direct read after write). In Table 1 the different types of disk-shaped optical media for two-dimensional data storage

Table 1. Methods of Two-Dimensional Data Storage on Disks

Symbol	Typical properties	Examples	Application of polymers
CD-ROM	not erasablenot rewritable	technology identical with audio compact disk (CD-DA)	substrate and information layer from polycarbonate (PC)
WORM	writablenot erasable	polymeric or glassy substrates with metal or alloy layer, dye-in polymer film	substrate $\theta \leq 51/4$ in.[a]: PC $\theta > 51/4$ in.: glass, partly PC
EOD	erasablerewritable	polymeric or glassy substrates with magnetooptical recording layer (MOR); phase change recording layer (PCR); photochromic dyestuff	substrate $\theta \leq 51/4$ in.: PC, partly glass $\theta > 51/4$ in.: not on the market

[a] 5 1/4 in. is a standard disk size.

are listed according to their construction, type, fundamental characteristics, examples of their implementation and use of polymers. Multidimensional data storage systems being currently developed are holographic data storage in which information is stored as a diffraction or as an absorption hologram or photochemical, respectively, photophysical hole burning (PHB). In holographic methods polymers are used as both matrix material and as storage media (see Holography). In PHB polymers are used as matrix material.

2. Planar Data Deposition (2-D Storage)

2.1. Data Storage with Prerecorded Information

CD-ROM disks are nearly identical to the well-known compact disk-digital audio (CD-DA; short CD). The information on a CD-ROM is stamped in the form of clearly defined pits on the disk surface during the disk's manufacture, using injection molding or injection stamping techniques. A metal stamper transfers the digital information to the disk's surface.

The digital information is represented by the position and length of microscopic pits on the surface of a CD-ROM that are arranged in a spiral track. A CD-ROM of 120 mm (4.75 in.) diameter has a gross capacity (unformatted) of about 600 MByte and a net capacity (formatted) of 540 MByte (ISO-Norm 9660), respectively. This is equivalent to 200,000 pages of text. The access time is between 200 and 600 ms. The data transfer rate of a standard audio CD player is 144 KB/s, but dedicated CD-ROM drives can transfer data at up to 300 KB/s by doubling the rotational speed of the disk.

Figure 1**a** schematically depicts a cut-out of a CD-ROM sector (1); the sketch shows the track-to-track distance (1.6 μm) and the width of a pit (about 0.6 μm). The pit length varies between 0.8 and 3.3 μm. The pit depth is 0.11–0.12 μm. Figure 1**b** shows the structure of the spiral grooves for tracking that are imprinted into the substrate material of CD-DA during manufacture. To read the stored digital information, low energy laser diodes (about 7 mW) are employed with emission wavelengths from 780 to 840 nm. As shown in Figure 2, the focused laser beam is reflected by the sputtered aluminum cover layer and received by a photodetector. In the process, the laser beam (φ (diameter) about 1 μ) is scattered in the pit area and weakened by interference, respectively, but reflected optimally in the flat areas in between. Thus, the digital data, which is coded with certain algorithms, can be read. CDs use bit-edge detection, ie, the high to low transition itself is responsible for the signal at the photodetector, registered as a 1 or as a 0, respectively.

The physical CD format has been recognized as an industry standard: all CD-ROMs are of the same size, and data are stored in the same way in the same physical format. Details are put down in the so-called Yellow Book (Philips/Sony).

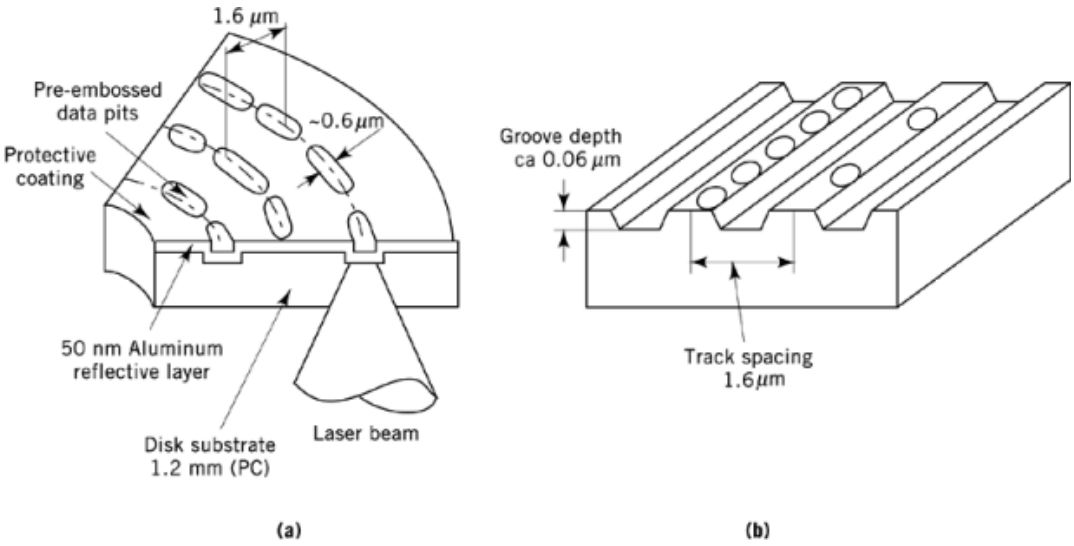

Fig. 1. Compact disk geometry: (**a**) CD-ROM, sector detail (1); (**b**) CD-DA, geometry of the tracks (grooves).

For the logical format of a CD-ROM, a standard has also been agreed on (High Sierra Proposal, normed as ISO 9660; extension rock ridge), which governs the storage of files and enables the common operating systems (Apple HFS, MS-DOS, UNIX, VMS) to access them.

Besides the established audio CD and CD-ROM, there are other variants of optical storage disks with imprinted information which differ in the way the data are processed.

The CD-I (compact disk-interactive) is a low cost alternative to the CD-ROM for the entertainment industry. CD-I is a subset of the CD-ROM standard data format. It allows the digital storage of data, audio, and video information in a form that permits rapid interaction with a computer. CD-I is compatible to CD-ROM and to CD-AD; θ = 120 mm. The definition of the CD-I format is put down in the Green Book (Philips/Sony).

CD-XA (CD-extended architecture) is the standard for CD-ROMs for data storage and compressed audio recording (up to four hours music in HiFi-stereo quality). The definition of the CD-XA format is also put down in the extended Yellow Book.

CD-R (CD-recordable) is a writable, nonerasable disk, also called CD-WORM or CD-WO (CD-write once). Permanent marks are produced by a focused laser beam. The definition of the CD-R format and of the erasable–rewritable EOD/MO-R format is put down in the Orange Book (Philips/Sony).

CD-V (compact disk-video) is premolded for both video and digital music; θ = 305 mm or θ = 203 mm. There is also a videoclip version (θ = 120 mm) for 22 min CD audio and 5 min of video information. CD-VEP (video extended play) θ = 200 mm, is recorded on both sides, whereas for CD-VLP (video long play) θ = 200 mm, one- or two-sided recording can be selected; max. 60 min video/side.

Not in the class of digital recording storage media are video CDs with diameters of 200 and 300 mm, respectively. These are storage disks for recording the analogue signal of videos and are of air-sandwich construction with two poly(methyl methacrylate) disks.

2.2. Writable, Nonerasable Data Storage

In many applications, data storage systems are required which enable the user to write data and text as well as in some cases digitized graphics and pictures. They should allow fast access to the stored information at all times. The information itself, however, may not be changed, erased, or overwritten. Examples for these

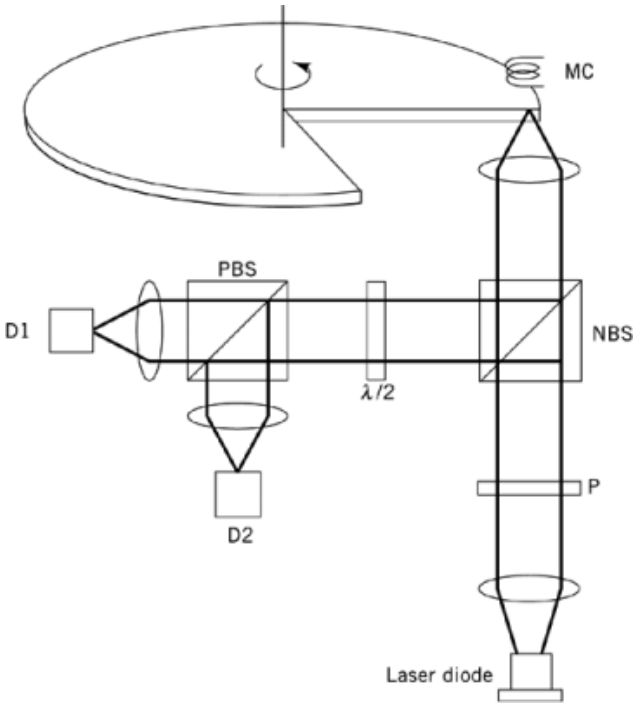

Fig. 2. A magnetooptical player (2). P=polarizer; MC=magnetic coil (for magnetooptical writing); NBS=neutral beam splitter; PBS=polarizing beam splitter. D1, D2=detectors for differential detection. The optical path also comprises tracking and focusing optics which are not shown here.

applications are mainly office files, especially those which require mandatory storage, protection against manipulation, and forgery-proof documents, eg, expense statements, payment and salary files, bank statements, employee files, or production instructions. In general, these storage systems could substitute for filing of documents on paper or archiving on microfiche.

The conditions of these target applications are fulfilled by WORM-disks. Apart from data compression on a small volume, WORM filing systems offer the advantage of fast access from the workplace at all times, including a simplified document search and retrieval strategy.

A WORM disk generally consists of two polycarbonate disks with 130 mm diameter in sandwich construction. The storage capacity of a WORM disk varies depending on the disk diameter, the manufacturer, the mechanism, and disk formatting. Currently, WORM disks of 5.25 in. format are offered with 2×235 MByte or 2×470 MByte capacity (double-sided), and of 12 and 14 in. format with capacities ranging from 1 to 4.1 GByte (double-sided). A breakthrough in WORM applications is the introduction of a WORM disk in CD format (so-called CD-WORM or CD-R; R = recordable), offering the possibility of using CD-WORM disks in customary, new generation CD players (multimedia operation).

A special implementation of the CD-R disk is the Photo-CD by Kodak which is a 5.25 in. WORM disk employing the dye-in-polymer principle for storage of up to 100 slides/pictures on a CD (after data compression) with the possibility of interactive picture processing.

WORM disks must fulfill the following requirements (3): high storage capacity ($>2 \times 10^7$ bit/cm^2), short access time ($<10^{-1}$ s), read back with high signal-to-noise ratio $\geq$47 dB, long shelf life of the information ($>$20 years), low storage costs ($\leq 10^{-7}$ \$/bit), low error rate (BER = bit error rate $\leq 10^{-12}$ bit, after error correction), and high reliability (MTBF = mean time between failure $>$ 2000 h).

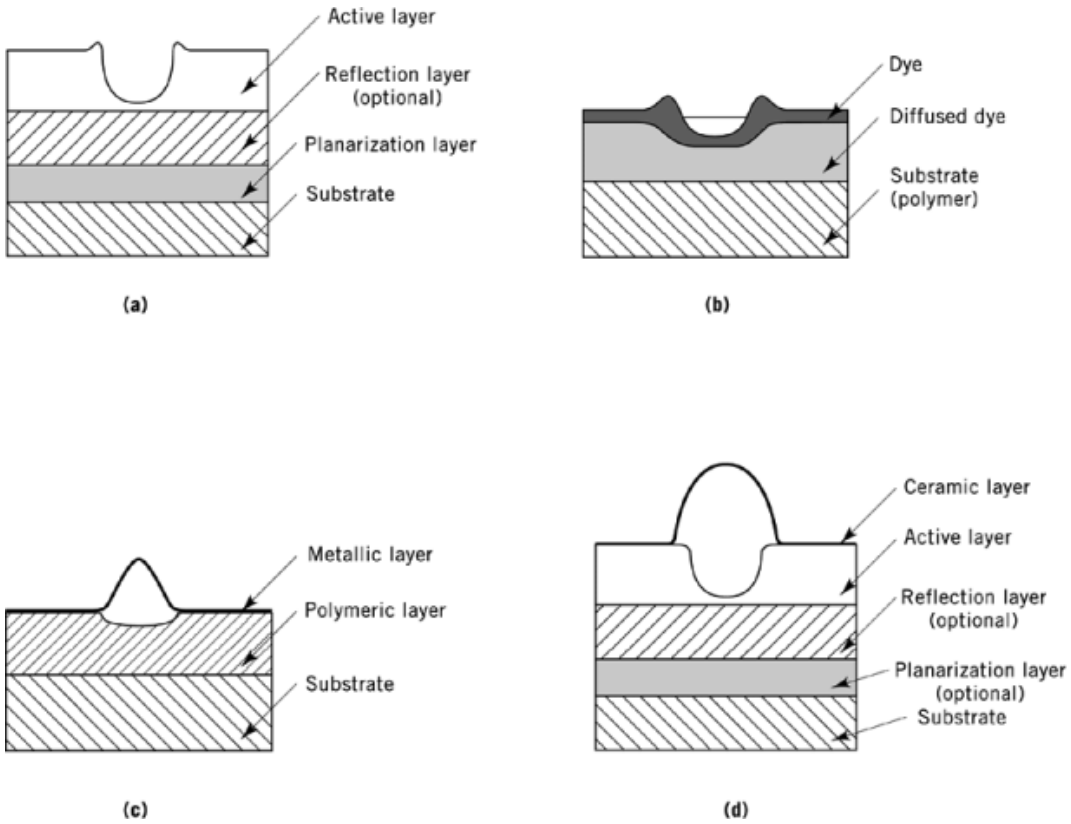

Fig. 3. WORM media: data writing techniques and typical layer construction (3): (**a**) ablative writing, DIP concept (4); (**b**) ablative writing, LIDA technique (5); (**c**) writing by bubble forming; (**d**) writing by bubble forming, layer arrangement after (6).

2.2.1. Writing Techniques

WORM disks differ depending on their data writing techniques, which can be divided into three classes (3): ablative writing, bubble forming, and phase change.

2.2.1.1. Ablative Writing. This technique involves burning or melting of pits. Holes may be burned into thin dye layers, preferably organic pigments. Burning of holes into thin metal alloy layers, eg, Te or Bi films is another method. Holes are burned into polymeric active dye layers, which contain light-absorbing additives tuned to the laser wavelength used (organic dyes or pigments, inorganic pigments, carbon black, etc). Especially good effects are achieved with a strong interaction between dyes and the polymeric binder, the dye-in-polymer (DIP) concept (4) (Fig. 3**a**). The melting of pits in connection with heat-induced diffusion of an organic dye into the polymeric binder is the laser-induced dye amplification (LIDA) technique (5) (Fig. 3**b**).

2.2.1.2. Writing by Bubble Forming. Bubble formation occurs under thin metal layers on polymeric substrate films, caused by local evaporation when hit by a focused laser beam (see Fig. 3**c**). Bubble formation occurs as in the DIP concept in dye-in-polymer films which are covered by a thin metal (mostly gold) or ceramic layer (6) (see Fig. 3**d**).

In variations of these first two methods, the information is written by creating holes/pits/bubbles of about 1 μm size with a laser (power 20–40 mW, impulse length about 50 ns). Reading is also done optically by laser (power about 0.5 mW) using the changed light reflection or scattering characteristics of these marked patterns.

Here it is advantageous to improve the efficiency of optical absorption and to improve the signal contrast significantly by an additional thin, metallic reflecting layer beneath the memory layer. These are called tuned optical structures.

The mechanism of hole- or bubble-forming in metal or dye polymer layers continues to be a subject of intensive investigation (7).

2.2.1.3. Writing by Phase Change. In an amorphous layer, crystalline marks are generated by local annealing with a focused laser beam.

2.2.2. Dyes for WORM-Disks

Regarding their memory layer, dye-in-polymer systems show advantages over metal layers in their higher stability, lower toxicity, lower heat conductivity, lower melting and sublimation temperature, and simpler manufacturing technique (substrate coating by sublimation or spincoating).

The following requirements need to be fulfilled by dyes or dye-in-polymer systems as active components in WORM-disks: high absorption capability at the wavelength of the write laser (wavelength 780–840 nm is low writing energy); defined threshold to avoid destructive reading; low heat conductivity parallel to the disk surface to yield focused pits, ie, high storage density, low toxicity, good solubility in solvents (eg, pentanol, hexanol) which do not attack the disk material (generally polycarbonate); and good film forming, ie, low cost manufacturing technique.

The GaAs laser used as light source emits at about 820 nm. Thus dyes in the actual sense are not needed; rather, ir-absorbers for the spectrum between 750–850 nm; little experience is available on this class of dyes, especially as far as their stability is concerned, although much work has been done in this area. Also, infrared sensitive dyes and pigments, used in electrophotography, may be very suitable for WORM disks (8).

To yield high storage densities, layer thicknesses in the order of the focused laser beam are necessary in the storage medium, measuring about 1 μm. In commercial WORM disks based on pure dye layers, layer thicknesses are even lower at about 0.1 μm. With thicknesses as low as these, it becomes difficult to ensure sufficient light absorption, so the dyes need to possess a high molecular extinction. A low heat conductivity of the storage layer is of equal importance; only layers with low energy dissipation yield small focused pits already at low write energies, and with that a high storage density.

The dyes used can be classified in four groups (3) as follows.

2.2.2.1. Methine Dyes. In this dye class, special importance has been gained by zwitterionic hydroxy squarylium dyes (9) (Fig. 4**a**) (10), the cationic dye SQS (squarylium core with thiopyrylium end group (11) (Fig. 4**b**), and the cationic polymethine tetra(dimethylaminophenyl)pentamethineperchlorate (TPMP) (11) (Fig. 4**c**) due to their favorable specific combination of characteristics: high optical absorption at the laser wavelength, high signal-to-noise ratio on reading, low error rate, and reasonable production cost. As an example, the reflectance R and the transmittance T of a 75-nm thick SQS film is plotted as a function of wavelength λ in Figure 5 (11).

In WORM disks, pentamethine and heptamethine are the materials of choice (see Cyanine dyes; Polymethine dyes).

2.2.2.2. Naphthalocyanine Derivatives. These dyes, which contain a naphthalocyanine skeleton as chromophore, show high absorption in the area around 830 nm, possess low melting points, and small heat conductivity. A disadvantage of the unsubstituated naphthalocyanine is its low solubility in organic solvents which do not attack the polymeric substrate material (generally polycarbonate); substituents improve solubility (see Phthalocyanine compounds).

The basic structure of a naphthalocyanine dye can be seen in Figure 6 (12). By varying the central atom Y, the organic (polymeric) group Z_p at the central atom, and the substituents X_m and X_n, an adjustment to the desired property profile, especially improved solubility, can be achieved. Naphthalocyanines with silicon

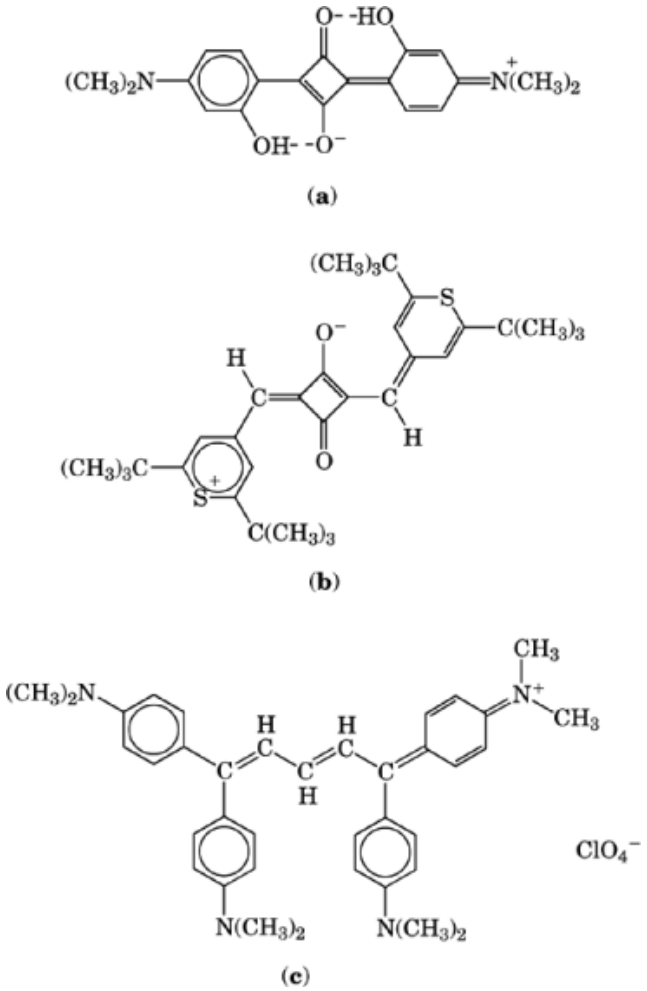

Fig. 4. Dyes for WORM media: (**a**) hydroxy squarylium (9, 10); (**b**) SQS=squarylium core with thiopyrylium end group (11); (**c**) TPMP= tetra(dimethylaminophenyl)pentamethineperchlorate (11).

as central atom evoke special interest, eg, the biaxially substituted silicon–naphthalocyanine (13) wherein the central **Si** bears two Z_p substituents and the rings are unsubstituted, ie, $X_m = X_n = H$.

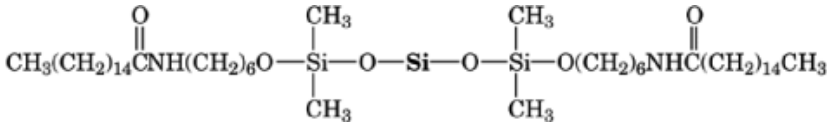

This dye shows high absorption at wavelengths between 780 and 830 nm, and a reflectivity of about 30%. This signal-to-noise ratio is about 50 dB with high consistency, even after 10^6 read cycles (14). A disadvantage is the high expenditure for the synthesis of these derivatives due to low yield (15).

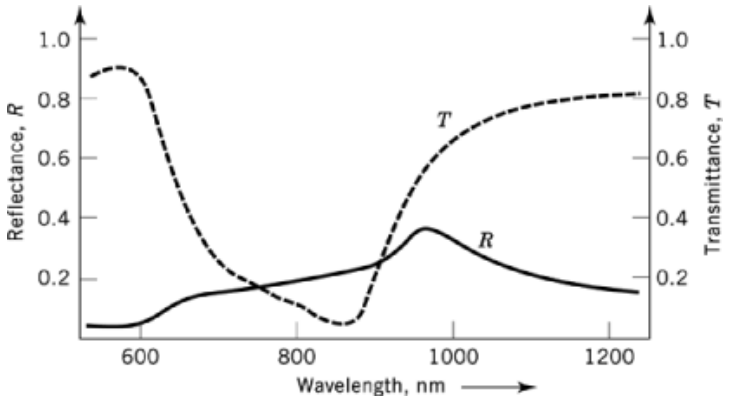

Fig. 5. Reflectance and transmittance spectra for a 75-nm thick SQS film (11).

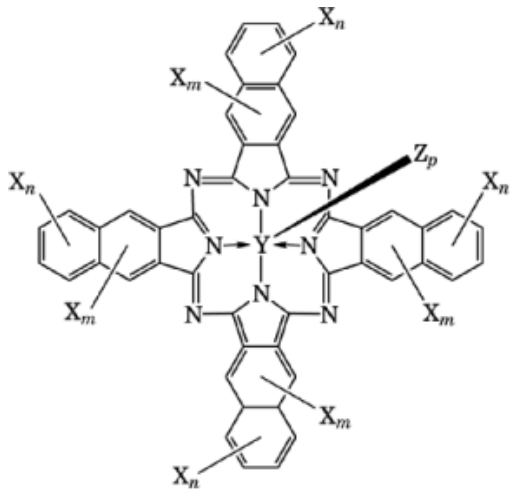

Fig. 6. Dyes for WORM media: phthalocyanine derivatives. The basic structure (12) of naphthalocyanine derivatives. Y= Si, Ge, Sn, Al, Ga, In, or a transition metal; Z_p=OR_1, $OSiR_2R_3R_4$, polymer. X_m and X_n represent substituents on the rings of the naphthalene system.

2.2.2.3. Naphthoquinone Derivatives. These dyes are generally not very colorfast and sometimes also fade. Anthraquinone derivatives have better properties (see Dyes, anthraquinone). New developments are based on compounds that combine the chemical structure of phenothiazine or phenoselenazine derivatives with benzoquinone or naphthoquinone units (16). These dyes show good chemical stability. Naphthoquinone derivatives have yet to find a practical application as dyes in WORM disks because of the high expenditure for synthesis due to low yields.

2.2.2.4. Metal Complexes. The importance of Ni complexes is based on their effectiveness as quenchers for singlet oxygen. Of disadvantage is their low colorfastness and their lower ir-reflectance compared to cyanine dyes (qv); therefore they are used in combination with suitable dyes. Numerous complexes are described in the literature, primarily tetrathiolate complexes of Pt or Ni, eg, dithiolatonickel complexes (3). Well known is the practical use of a combination of benzothiazole dyes with nickelthiol complexes in WORM disks (Ricoh, TDK) (17).

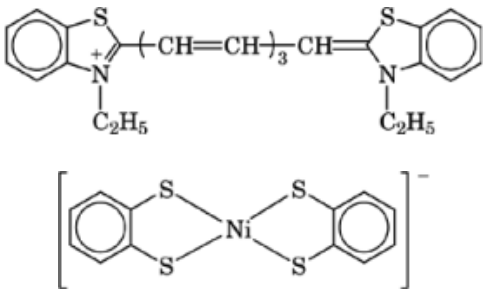

2.3. Erasable, Rewritable Optical Data Storage

The principal use of CD-ROM and WORM disks is essentially substitution of data storage on paper or microfiche. Conservative estimates number the worldwide use for data storage by paper at 91%, microfiche at 4%, and in electronic media at 5%, of which 4% are magnetic and 1% optical media (18). CD-ROM is being used as an electronic counterpart to print media; the WORM disk presents itself more and more as a substitute for paper to store archivable, forgery-proof documents.

Erasable optical disk (EOD) systems, on the other hand, are challenging classic magnetic media in some areas of application, primarily magnetic tape and the hard disk, but mostly optical media complement magnetic media.

In spite of the enormous advantages of erasable optical disks (higher storage density, trouble-free removable media, easy handling, low susceptibility to interference, low cost per bit), their market share of the whole mass storage market is relatively small as of the mid-1990s, contrary to earlier optimistic prognoses. This is less due to the specific disadvantages of the EOD compared to magnetic hard disks (longer access time, lower write/read speed), but primarily to a higher price.

High demands are made on erasable, rewritable optical data storage: high storage density ($\geq 2 \times 10^7$ bit/cm^2), short access time ($\leq$30 ms), reading with high signal-to-noise ratio ($\geq$47 dB), high data transfer rate ($\geq$0.7 MByte/s), high number of read/write cycles ($\geq 10^7$), long guaranteed shelf life of data ($\geq$10 years), low susceptibility to dirt and disturbances, trouble-free removable media, low cost per bit ($\leq 10^{-7}$ \$/bit), low bit error rate (BER $\leq 10^{-12}$, after correction), and high reliability (MTBF $\geq 10^5$ h). EOD of the MO-R (magnetooptical recording) principle that have been on the market for several years, and the more recently introduced EOD of the PC-R (phase change-recording) principle, fulfill these requirements to a large degree, except for the long access time (20 to 80 ms) that should still be decreased. The data transfer rate can be raised, for example by increasing the rotation speed of the disk and/or the use of laser diode arrays.

2.3.1. Magnetooptical Recording

In a simplified way, a magnetooptical recording (MO-R) system can be regarded as a CD recorder using polarizing optics, a laser of controllable intensity, and a magnetic coil (see Fig. 2) (2). Currently, near ir-laser wavelengths of 780–820 nm are used, but red and blue recording which enables higher storage densities has been discussed. A disadvantage of MO storage technology in comparison to magnetic hard disks is the longer average access time: typically 30 ms, as compared to 10 ms. This is caused by the mechanical inertia of MO write/read heads. Because of the small track pitch, great demands are placed also on the actuator which controls head motion; to reduce the access time, intensive research is under way to produce lighter integrated optical heads.

As storage medium a (pregrooved) disk containing a hard magnetic layer is used where the information is stored in magnetic domain patterns. Currently used track pitches range from 1.35 to 1.6 μm. The principal advantages of MO recording in comparison to magnetic recording on hard disks are the removability of the disks and the immunity to head-crashes, the insensitivity against dirt, dust, fingerprints, etc (well known from

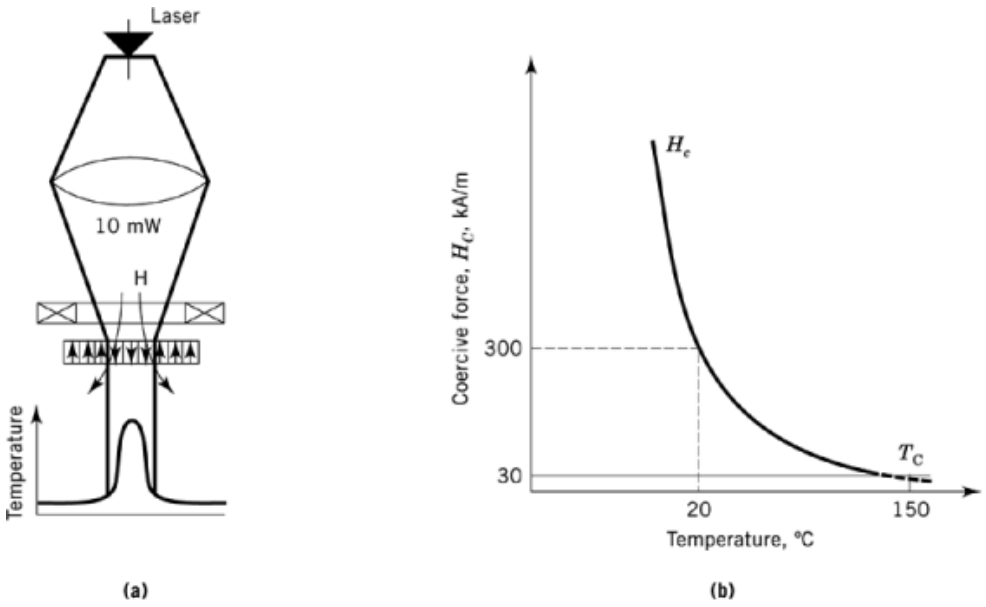

Fig. 7. Thermomagnetic recording. (**a**) A focused laser beam generates a thermal profile in the magnetic layer. (**b**) The coercive force in the layer is reduced and its magnetization can be reversed by a small magnetic field, here 30 kA/m. At room temperature, the coercive force is high and the written domains are stable.

audio CDs), which stem from the larger distance both of the optical head and the magnetic coil to the disk. The removability of the disks combined with high area densities leads to high total data capacities of MO recording systems. In 1994, 1.3 Gbyte storage capacity on 5.25 in. disks can be achieved for a track pitch of 1.35 μm.

In the thermomagnetic write process (Fig. 7), a focused laser beam with a typical power of 10 mW locally heats the magnetic layer to its Curie temperature, where the spontaneous magnetization and the coercivity vanish. During cooling, the magnetization in the heated spot can be reversed by a small magnetic field (demagnetizing field of the layer itself and externally applied field), creating a magnetic domain. A cylindrical domain written in this way can be regarded as a frozen-in magnetic bubble and has correspondingly been treated both theoretically (19, 20) and experimentally (21, 22). Because of the high coercivity at room temperature, the data stability is excellent.

The read process utilizes the polar magnetooptical Kerr effect: the polarization plane of the reflected light is rotated clock- or counterclockwise by a perpendicular magnetization (up or down) in the film according to the domain pattern (Fig. 8). The minimum usable domain size is determined by the optical resolution during read-out. A typical size is 1 μm, which corresponds approximately to the diameter of the laser spot. For the materials used, the magnitude of the Kerr rotation is only 0.2 to 0.3°. Consequently, the read-out signals are fairly small. They can, nevertheless, be detected with a good signal-to-noise ratio (SNR), if the noise generated by the reflection and polarization reflections at the disk can be kept low. This is a necessary but not sufficient condition. The key for obtaining a high signal-to-noise ratio is the domain regularity. MO recording systems require a SNR >45 dB; optimized high performance disks achieve 60 dB.

Two write methods are in use: magnetic field modulation (MFM) and laser modulation (LM) (2). With MFM, the whole track is heated by a laser beam of constant power and the magnetic field is switched according to the signal. Therefore, MFM is like a laser-assisted magnetic recording. This results in crescent-shaped domains like those shown in Figure 8. After writing, all old domains have been erased and only new information is on the track (direct overwrite, DOW). The data rate is limited by the inductance and heating of the magnetic coils.

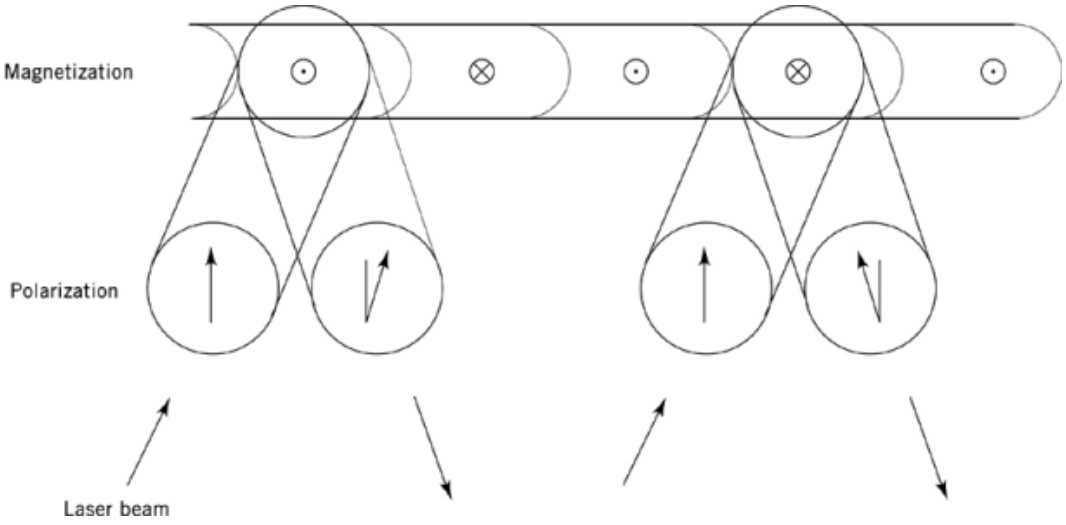

Fig. 8. Principle of the magnetooptical read-out of domain patterns by the polar Kerr effect. The polarization plane of the incoming laser beam is rotated clock- or counterclockwise according to the orientation (up or down) of the magnetic moments.

Practically achieved data rates are about 0.7 MByte/s (23). Therefore, in order to make the coil smaller, there have been attempts to reduce the necessary write field; theoretical limits are discussed in Reference r24. One possibility is to decrease the distance to the MO layer by placing the coil on the layer side of the single-sided disk. Another possibility is to make the MO layer more field-sensitive, eg, by covering it with a soft magnetic capping layer (25, 26).

With LM, the magnetic field is kept constant while the laser is switched according to the signal. Because only the laser power is modulated, possible data rates are higher than for MFM. They are limited by the present coding electronics to about 2 Mbyte/s, the same as for magnetic hard disks. Therefore, LM is the preferred mode for data storage applications. The main drawback of this method is that only new domains are written but no old information is erased. Whole sectors have to be erased in a separate run before new information can be stored (no DOW). A solution to this problem is the use of multilayers.

From the write and read process sketched so far, some requirements for MO media can be derived: (*1*) a high perpendicular, uniaxial magnetic anisotropy K_u in order to enable readout with the polar Kerr effect; (*2*) a magnetooptically active layer with a sufficient figure of merit $R{\cdot}\theta_K$ where R is the reflectivity and θ_K the Kerr angle; (*3*) a Curie temperature between 400 and 600 K, the lower limit to enable stable domains at room temperature and the upper limit because of the limited laser power for writing.

The coercivity of a material is determined by the coefficient $K_u/2M_s$ (27, 28). If it is sufficiently high, demagnetizing effects during writing are avoided and square hysteresis loops ensured. Therefore, it is advantageous that the magnetization of the MO layer is not too high between its Curie temperature and room temperature.

2.3.1.1. Materials for MO Media. The materials classes best suited for MO media are RE-TM alloys, Co/Pt multilayers, and ferrites. The quality of disks is mainly characterized by the signal-to-noise ratio (SNR).

Rare-Earth Transition-Metal Alloys. Amorphous thin films consisting of rare-earth–transition-metal (RE-TM) alloys were prepared in 1972 by coevaporation of Gd and Fe in the compositional range 15–94 atomic % Fe (29). In 1973 it was discovered that sputtered Gd–Co and Gd–Fe films contain striped and

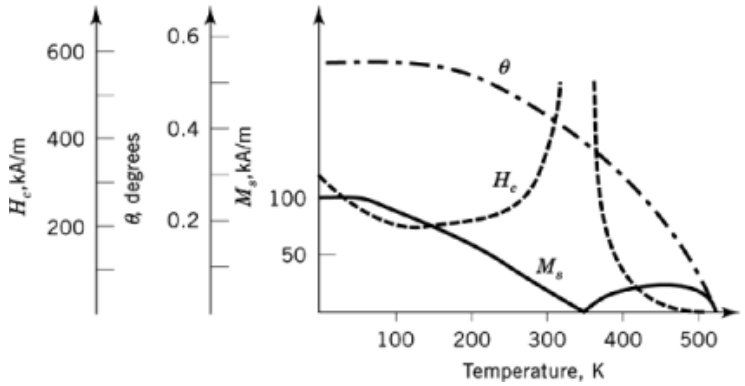

Fig. 9. Temperature dependences of the saturation magnetization M_s, the coercivity H_c, and the Kerr rotation θ_K for a 50-nm $Gd_{0.24}Tb_{0.01}Fe_{0.75}$ film.

cylindrical domains indicating perpendicular anisotropy, and it was demonstrated that these films are suited as media for MO recording (30). Since then, RE-TM alloys have emerged as the material of choice for erasable optical recording. This preeminence results from a fundamental understanding of the basic magnetic material properties of RE-TM alloys as well as their deposition and optical recording properties and processes. An extensive review of the magnetism of amorphous RE-TM alloys can be found (31). The specific aspects relevant for recording are treated in References 32–39. A review (40) emphasizes among other things the domain dynamics and magnetization reversal in RE-TM films and RE-TM periodic multilayers.

RE-TM films can be prepared in a wide compositional range by electron beam evaporation, r-f (radio frequency) and d-c (direct current) diode, or magnetron sputtering (3). Magnetron sputtering is the method of choice for deposition, because it allows deposition at low argon pressure which gives optimum micromagnetic properties and high deposition rates for efficient production. The main deficiency of these materials is their corrosion due to the presence of rare-earth elements. Protective layers are therefore necessary.

The magnetic moments of the heavy RE elements (Gd, Tb, Dy, etc) are coupled antiparallel to the magnetic moments of the TM elements (Fe, Co, etc). The $RE_{1-x}TM_x$ alloys are therefore ferrimagnetic below their Curie temperature (T_C). The heavy TM moments form one magnetic sublattice and the RE moments the other one. In contrast, the light RE moments (eg, Nd, Pr) couple parallel to the moments of TM. The RE spin is always antiparallel to the TM spin, but for the light RE elements, the orbital momentum is coupled antiparallel to the spin and larger than the spin.

The temperature dependence of some key magnetic properties of a typical ferrimagnetic RE-TM composition is shown in Figure 9. The temperature at which the opposite magnetizations of the sublattices are equal in magnitude and the net magnetization is zero is called the compensation temperature (T_{comp}). At this temperature, the coercive field H_c needed to reverse the magnetization becomes infinite. In comparison, the MO effects at 800 nm wave length (Kerr rotation angle θ_K), which are mainly due to the TM sublattice, are a continuous function of temperature. The presence of a compensation temperature can be used to control H_c and M_s. In the temperature range where the thermomagnetic switching process takes place, the maximum value of M_s above T_{comp} is approximately proportional to $T_C - T_{comp}$. A practical compensation temperature is found in a very narrow compositional range around 75 atomic % TM.

Figure 10 presents the Curie temperature (T_C) vs the TM-content (x) for Co- and Fe-based binary alloys. Alloying rare-earth elements with small amounts of transition metals ($x < 0.2$) leads to a decrease in Curie temperature. This is particularly obvious in the Gd–Co system where it corresponds to a nonmagnetic dilution similar to that of Cu (41, 42). This indicates that TM atoms experience no exchange coupling unless they are

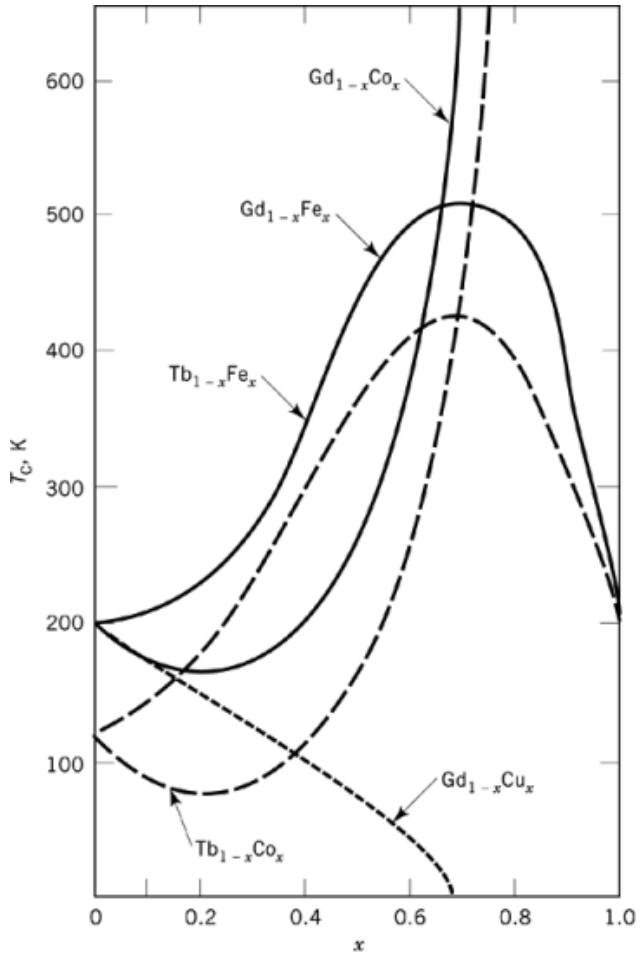

Fig. 10. Compositional variation of the Curie temperature (T_C) vs the TM content (x) for Co- and Fe-based binary RE-TM alloys. In the range of practical interest (about 75 atomic % TM), T_C is nearly independent of the Fe content, but strongly dependent on the Co content (about 7 K/atomic %).

surrounded by a minimum number j of other TM atoms. The critical number is $j = 5$ for Fe and $j = 7$ for Co. The steep increase of T_C for Co-based alloys with x about 0.7 is based on this effect.

For Fe-based alloys, a maximum in $T_C(x)$ can be found at $x = 0.7$. When x is increased further, the low T_C of amorphous Fe (approximately 200 K) is approached, due to the very strong influence of the structural disorder on the Fe-Fe exchange interaction leading to sperimagnetic order (43). The Curie temperature of Fe-based alloys can be increased by adding a small amount of Co. This effect allows a very fine tuning of the Curie temperature in the recording relevant region.

The magnetooptic spectra of amorphous RE-TM alloys are determined by contributions from both the TM and RE (44). In the ir wavelength region (used in today's MO-R), the MO effect stems mainly from the TM. In the visible and especially in the uv, a contribution of RE has to be taken into account. The RE contribution adds to the TM effect for the light RE, Nd and Pr, but reduces it for the heavy RE, Tb and Dy.

There have been many experimental investigations on the uniaxial (perpendicular) anisotropy constant K_u in amorphous RE-TM films. A synthesis of much of the existing data has been attempted in Reference 45. A

Table 2. Magnetic Fundamentals of Rare-Earth Transition-Metal Thin Films

Property	$Gd_{1--x}Fe_x$	$Tb_{1--x}Fe_x$	$Dy_{1--x}Fe_x$	Desired
compensation point at 295 K	$x = 0.77$	$x = 0.75$	$x = 0.82$	
dT_{comp}/dx,[a] K/at. %	114	30	23	medium
anisotropy[b] K_u, 10^5 J/m^3	−0.2	+6	+1	>+0.3
T_C, K	500	405	340	450
dT_C/dy,[c] K/at. % Co	7	7	10	

[a]Change of compensation temperature with composition is dT_{comp}/dx.
[b]Positive value of K_u indicates perpendicular anisotropy.
[c]Increase of Curie temperature when adding Co is dT_C/dy.

pseudocrystalline or cluster model was proposed based on the idea that the short-range order in the amorphous state is similar to a relaxed crystalline one which in the compositional range around $RE_{0.25}$–$TM_{0.75}$ consists of a layering of TM-planes and RE-rich planes. It is consistent with the observed coordination numbers in amorphous films. Though there is no direct evidence of such structural units, it can be said that the model is able to explain the known experimental results on the effects of composition, substrate temperature, annealing, and bombardment during sputter deposition on the resulting magnetic anisotropy.

Extended x-ray absorption fine structure measurements (EXAFS) have been performed to investigate the short-range structure of TbFe films (46). It is observed that there is an excess number of Fe–Fe and Tb–Tb pairs in the plane of the amorphous film and an excess number of Tb–Fe pairs perpendicular to film. The increase of K_u with the substrate temperature for samples prepared by evaporation is explained by a rearrangement of local absorbed atom configurations during the growth of the film (surface-induced texturing) (47).

In Table 2 the magnetic fundamentals of the three binary systems Gd–Fe, Tb–Fe, and Dy–Fe relevant for recording are listed, together with the parameter values required for recording (37, 39). These alloys are ferrimagnetic, exhibiting for a certain compositional range a compensation temperature T_{comp} at which the net magnetization is zero. In order to get low magnetizations above room temperature, which is necessary to get a high T_C and to suppress subdomain formation due to demagnetizing effects, a compensation temperature around room temperature is favorable. This is obtained for about 75 atomic % Fe.

None of the binary compounds with this composition is well matched to the needs of MO recording. Gd–Fe has too high a Curie temperature and has an in-plane anisotropy. T_C is too low for binary alloys such as Tb–Fe and Dy–Fe. Co-based alloys which exhibit a T_{comp} close to room temperature have too high a Curie temperature. Practical MO RE-TM alloys are therefore ternary: GdTb–Fe, where the Tb introduces perpendicular anisotropy (48) increasing the coercivity, and decreasing T_C; Tb–FeCo (49) and Dy–FeCo, where the Co increases T_C and the Kerr rotation angle, θ_K.

Each of the systems has an optimum distance T_C–T_{comp} for which the SNR has a maximum. For Tb–FeCo this is at about 220 K (50), corresponding to 23–27 atomic % Tb and for Dy–FeCo at about 120 K (51), corresponding to 25–30 atomic % Dy. The corrosion resistance of the compositions can be improved by adding a few atomic % of, eg, Cr, Ti, Nb, In, or Pt. These metallic additives have some impact on the magnetic properties of RE-TM alloys (45). K_u is reduced to some extent and, especially for 3*d*-additives, the TM moment is decreased. Therefore, the RE-TM composition must be reoptimized when dopants are added.

Pt/Co Periodic Multilayers. Since the discovery of perpendicular magnetic anisotropy in periodic Co/Pd multilayers (ML) (52), many investigations have been carried out on similar structures with alternating ultrathin Co/X layers with X = Pd (53, 54), Pt (53–55), and Au (56). The elements Pd and Pt are magnetically polarizable by Co and the multilayers have very similar magnetic properties. For properly chosen thicknesses of the individual layers, the MLs exhibit perpendicular anisotropy and are therefore principally suited for MO recording. The big advantage of such systems is their high chemical stability, allowing simple stack designs

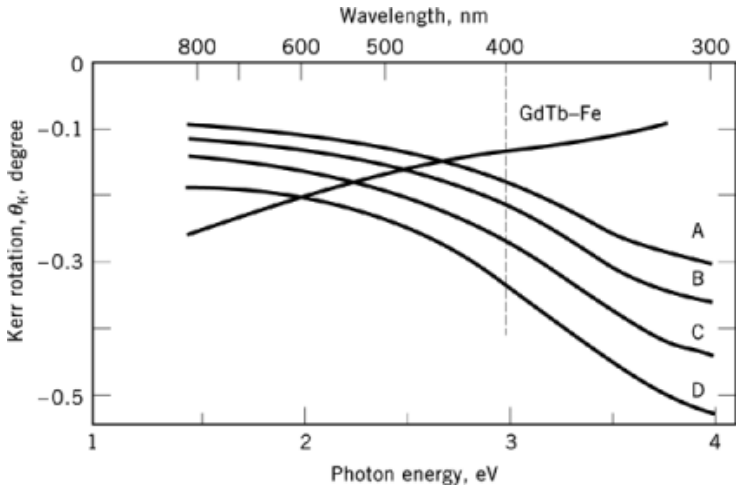

Fig. 11. The spectral dependence of the polar Kerr rotation for GdTb–Fe and for a series of Co/Pt multilayers with t_{Co}=0.36 nm and with A, t_{Pt}=1.94 nm; B, 1.63 nm; C, 1.28 nm; and D, 1 nm. Total thickness of all MLs is about 42 nm. Therefore, the Co content increases with decreasing t_{Pt} (adapted from Ref. 58).

without protective layers. In order to optimize the reflectivity, however, at least one dielectric layer between the substrate and the MO layer is needed. Co/Pt MLs are practically most important, because they exhibit the largest Kerr effect.

The magnetic properties of Co/Pt MLs depend on the thicknesses of the individual layers, t_{Pt} and t_{Co} (57). For $t_{Co} < 1.2$ nm, the axis of easy magnetization is perpendicular to the surface, as desired for MO recording. The maximum anisotropy is found for $t_{Co} = 0.4$ nm, corresponding to two atomic layers. Square hysteresis loops with 100% remanence are observed for $t_{Co} < 0.5$ nm and a total ML thickness of about 20 nm. A practically used configuration is, eg, 14× (0.4 nm Co +1.2 nm Pt). The information in these media is magnetically stored in about 30 layers of magnetic Co atoms.

The Kerr rotation angle (θ_K) of Co/Pt MLs increases in the ir and visible regions with increasing Co content. In the blue wavelength region it is larger than that of GdTb–Fe (Fig. 11) (58). The maximum of θ_K at 4.2 eV can be ascribed to a magnetooptic effect of Pt, where Pt is polarized by adjacent Co atoms (59). The Curie temperature decreases with increasing t_{Pt}. In Figure 11, sample D (t_{Pt} = 1 nm) has $T_C = 390^\circ$C and sample A (t_{Pt} = 1.94 nm) has $T_C = 300^\circ$C. For MO media, a compromise between high Kerr rotation and low write power must therefore be found.

Evaporated MLs exhibit a higher coercivity than Ar-sputtered films (sputtered at low pressures) and result also in the best recording results (60). With Ar-sputtering, the growing layer is exposed to a bombardment of reflected argon atoms with an energy of about 100 eV. This seems to enhance the surface diffusion, leading to sharp interfaces, but a distributed texture with twins. The energies for evaporation (about 0.2 eV) and Xe sputtering (about 1 eV) are lower, resulting in a rougher interface (1 nm roughness as compared to 0.3 nm for Ar-sputtering) (60). Increasing the argon pressure (such that the vapor species are thermalized) mostly induces a coarser, granular microstructure with voids correlated with an increased coercivity but a reduced anisotropy of the multilayers. In the low energy processes, a superior [111]-texture is observed, which is probably due to less nucleation and a more rigorous nuclei selection. The recording results for Kr-sputtered MLs are similar to those for evaporated MLs.

K_u can also be increased by suitable dielectric underlayers that also may serve for optical enhancement, eg, ZnO and In_2O_3 (61). They improve the [111]-texture because the [002]-planes of these materials grow in

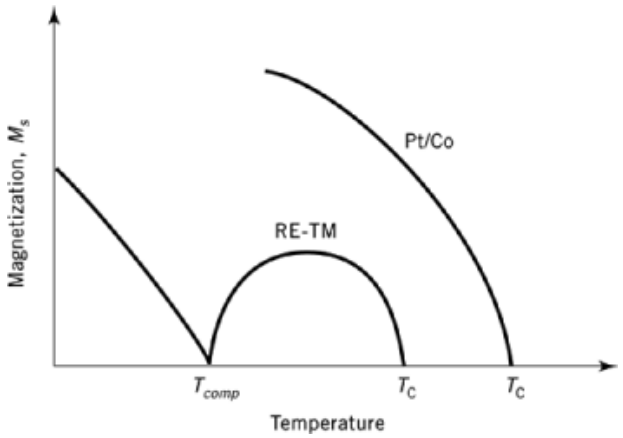

Fig. 12. Temperature dependences of the magnetization M_s, one curve typical for ferrimagnetic films, eg, RE-TM or garnets, the other one typical for ferromagnetic Co/Pt multilayers (39). T_{comp}=compensation temperature; T_C=Curie temperature.

parallel to the substrate surface; ZnO has in addition a small misfit ($<2\%$) to Pt/Co. These layers increase, however, the noise of the disks, probably due to polarization fluctuations.

As in the case of RE-TM alloys, the properties relevant for recording are determined by proper material selection and by the preparation process.

Comparison of RE-TM films with Pt/Co Multilayers. In Figure 12 the temperature dependence of the magnetization is schematically shown for a ferrimagnetic alloy (eg, amorphous RE-TM films) in comparison to a ferromagnetic metallic multilayer (39). The magnetic properties of Pt/Co multilayers are less favorable for MO recording than those of RE-TM films. First, they exhibit a higher Curie temperature ($>300^\circ$C) implying less thermal sensitivity in recording which is only partly compensated by their smaller film thickness. Therefore, there are efforts under way to reduce the Curie temperature without reducing the Co content, eg, by adding Os or Re to Co (62). Second, they do not have a compensation temperature, leading to a high magnetization in the temperature range of domain formation. Due to demagnetizing effects, this favors subdomain formation during writing and stability of residual domains during erasing. Therefore, higher magnetic fields are needed for writing and erasing in comparison to RE-TM-based disks (63).

An advantage of Pt/Co ML in future blue recording is their higher Kerr rotation in the visible wavelength region leading to a higher figure of merit (FOM). The purpose of blue recording is to get smaller domain sizes, but a higher FOM does not always lead to a higher signal-to-noise ratio (SNR). The signals and different noise levels expected for the two media classes are schematically depicted in Figure 13, for the case that the system noise is negligible.

If the predominant noise already stems from the unwritten disk and is not caused by magnetooptic effects, a higher signal proportional to $R{\cdot}\theta_K$, with R being the reflectivity of the layer, will indeed lead to a higher SNR. From the optical and magnetooptical constants a 3 to 6 dB higher FOM can be expected for Pt/Co. Results reported so far in the literature are related to this disk-noise limited range, and a few dB higher SNR is reported for Pt/Co in comparison to RE-TM. Examples are given below, where dl designates the length of the recorded domains and wl the laser wavelength used. The results for RE-TM disks obtained under the same recording conditions are given in parens.

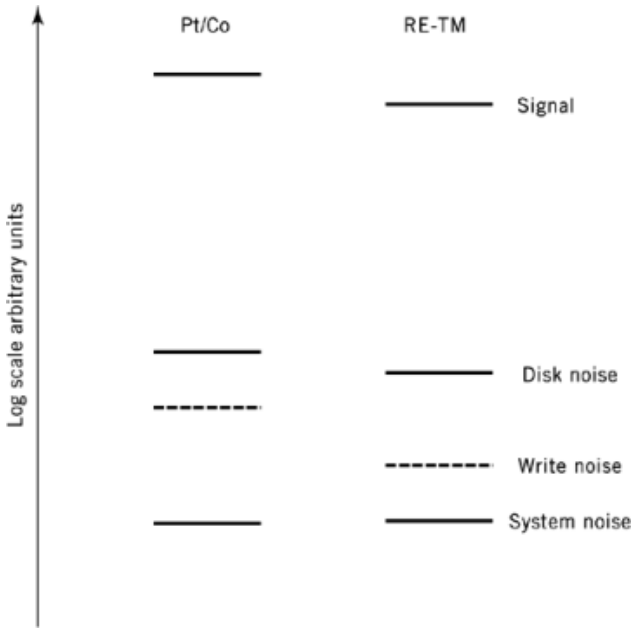

Fig. 13. Expected signal and noise levels for RE-TM alloys and Pt/Co multilayers (schematic). The total noise entering the SNR is the sum of the system noise, disk noise, and write noise. The system noise is electronic noise and photon shot noise and is comparable for disks with the same reflectivity.

SNR, dB, for ML	*dl*, μ	*wl*, nm	Reference
40 (38 dB for GdDyFeCo)	4.0	488	64
30 (24 dB for TbFeCo)	0.5	488	65
40 (37 dB for GdTbFe)	0.38	458	66
30 (20 dB for TbFeCo)	0.3	488	67

If the disk noise is suppressed by improved manufacturing procedures, the predominant noise is expected to be caused by irregularities of the domain boundaries (domain jitter), and signal and noise are equally enhanced by a higher FOM and the SNR is not improved. In this range (write-noise limited region) which extends for disks and ir recording up to about 58 dB, RE-TM based disks might have an advantage because of their finer microstructure. This is most important for domain edge recording.

If the microstructure becomes ever finer by improved deposition technology, the domain irregularities should diminish. The SNR is limited by the shot noise of the laser source and is equal to $R{\cdot}\theta_{\mathrm{K}}^2$. In this region a high θ_{K} is of great value.

Magnetic Oxides. Mixed oxides of ternary iron and other metal ions that crystallize in a structure of spinel, garnet, or hexagonal type have also been investigated as MO media. These materials are discussed in References 68 and 69. The general composition of spinel is MFe_2O_4 where M = Co, Mn, Ni, Zn, and others (70). An example optimized for high Kerr rotation is $CoFe_2O_4$. Rare-earth iron garnets (RIG) have the formula $R_3Fe_5O_{12}$ where R = Y, Gd, Tb, Dy (71, 72). An example for a hexaferrite (73, 74) is $Ba(CoTiFe)_{12}O_{19}$.

Promising candidates for MO recording among the ferrites are ferrimagnetic garnets of composition $Dy_{3-x}Bi_xFe_{5-y}(Ga, Al)_yO_{12}$ (71, 72). The primary effect of Bi is a strong enhancement of the MO effect. Due

to a strong intrinsic magnetostrictive effect, Dy enhances the perpendicular anisotropy, which is primarily stress-induced by the magnetostrictive effect.

These materials can be deposited by pyrolysis or by RF sputtering onto glass or garnet substrates. A deficiency of garnets and oxides is their high crystallization temperature ($>400^{\circ}$C) excluding polycarbonate (PC) as substrate material and making mass production difficult. Amorphous layers with garnet composition are paramagnetic at room temperature. The films become polycrystalline by *in situ* deposition on heated substrates or by post-annealing.

The garnets exhibit a high chemical stability (advantage over RE-TM), suitable magnetic properties, and high magnetooptical effects at shorter wavelengths (no clear advantage). In particular the presence of a compensation temperature allows tailoring of the magnetization and coercive field similar to RE-TM alloys (see Fig. 12), which is an advantage over Ba-ferrites and Pt/Co ML. Optimized disk structures of a 230-nm garnet film sputtered onto single-crystalline GdGa–garnet substrates have shown a SNR of 54 dB at 514 nm wavelength for a domain length of 1.4 μm (75).

The magnitude of H_c, however, is determined by the stress-induced uniaxial anisotropy and by the grain size. The latter has to be small (<50 nm) to achieve high H_c but also noise levels must be sufficiently low. The polycrystalline nature of garnet films and thus the sensitive dependence of the grain size and its distribution on the deposition parameters is one of the crucial aspects of garnets for MO recording. Any irregularities in the morphology of the films lead to a drastic increase of the media noise reducing the SNR.

2.3.1.2. Exchange-Coupled RE-TM Layers. It is difficult to obtain RE-TM thin films that exhibit all the desired magnetooptic and micromagnetic properties. In most cases, the optimization of one property adversely affects another property. New and interesting possibilities in this regard utilize sandwich structures of two or more RE-TM films (exchange-coupled layers, ECLs) with different magnetic properties. One layer (the storage layer, *s*) can, eg, be optimized toward high coercivity for storage, and the other one (*r*) toward high Kerr rotation for read-out. Examples are [GdFe(*r*)/TbFe(*s*)] (73, 74, 76) or [$Nd_{10}Tb_{20}(FeCo)_{70}$/$Nd_{5--10}$TbFeCo] (77). For a trilayer stack [200 nm $Tb_{18}Fe_{49}Co_{33}$(*s*)/10 nm $Nd_{18}Co_{82}$(*r*)/5 nm $Tb_{18}Fe_{49}Co_{33}$] (78), a high coercivity of about 159 kA/m (2 kOe) and $\theta_K = 0.37$ to 0.46° has been reported.

The most spectacular applications of ECLs are the possibility of direct overwrite (DOW) with laser modulation (79, 80) and of magnetically induced superresolution (81, 82). The stacks comprise at least a storage layer *s* and a bias layer *b*. For both applications, the storage layer *s* has the lower T_C and the higher H_c at room temperature when compared to the bias layer *b*. At room temperature, *b* is homogeneously magnetized (initialized) by an external permanent magnet ($H_{initial}$ is about 400 kA/m (5 kOe)).

DOW is achieved by switching the laser power between two levels. For erasing, the double layer is heated up to the Curie temperature of layer *s*, so that *b* remains unchanged and *s* is initialized locally during cooling due to an exchange coupling to *b* (avoiding a magnetic interface wall). New domains are written first into *b* by switching the laser to the higher level and copied to *s* during cooling.

When used for superresolution, the laser beam is incident on *b*, which hides the domains in *s*. During read-out, *b* is heated and the domains in *s* are copied to *b*. The optical system sees only the overlap area between the laser spot and the temperature profile which is lagging behind, so that the effective resolution is increased. Experimentally it is possible to double the linear read-out resolution, so that a four times higher area density of the domains can be achieved when the higher resolution is also exploited across the tracks. At a domain distance of 0.6 μm, corresponding to twice the optical cutoff frequency, a SNR of 42 dB has been reached (82).

Stability of Domains. In bilayers used for DOW or superresolution, the bias layer is homogeneously magnetized in the ground state after a complete write or read cycle, whereas the storage layer contains magnetic domains leading to magnetic interface walls between the two layers. For the domains to be stable, the wall energy density σ_w has to be lower than the coercive (area) density $2 \cdot H_c M_s \cdot d$ of both layers (thickness, *d*).

In order to achieve stable storage in exchange-coupled layers, different stack designs and material compositions have been used. By increasing the thickness of the bias layer, its coercive energy is proportionally increased; the thermal sensitivity of the stack, however, is decreased. As an example, for Tb–FeCo(s)/TbDy–FeCo(b) a thickness of the bias layer b of 150 nm was reported (83). Instead of increasing the coercive energy, σ_w can be decreased by tuning the composition (84, 85) properly or by intermediate layers.

Intermediate layers reducing the wall energy can be magnetic with low K_u or even possess an in-plane easy axis (86–88), so that the core of the wall is situated in this layer for a minimum energy configuration. This has been achieved with, eg, 3–6 nm Nd–FeCo (89) or with an interface nitride layer (1.5–2.2 nm Tb–FeCoN) (90). The intermediate layer can also be a nonmagnetic layer, softening the exchange between the two magnetic layers (eg, Pd) (91).

The trilayer configuration is a considerable improvement over the original concept of DOW with ECLs. A reduction of $H_{initial}$ to 200 kA/m (2.5 kOe) has been achieved because the magnetic walls, which have to be created during initiation, have a lower σ_w (92).

Another significant achievement has been obtained with a quadrilayer stack, where the initializing of b is taken over by the two additional layers, so that an initializing permanent external magnet is no longer necessary (93–95). The additional initializing layer i has a T_C above the writing temperature and carries a permanent magnetization. The switching layer is situated between i and (b/s). Its Curie temperature is below the writing temperature but above room temperature, such that i decouples magnetically from b during writing but initializes b during cooling.

Interface Walls and Domain Formation. The existence of a macroscopically large interface wall between two magnetic layers gives rise to new effects in the domain formation process that are not possible in single layers (96, 97). The energy of the wall can be determined by reversal experiments (98, 99). The main feature is a possible vertical motion of the interface wall across one layer, which can also be a mechanism to destroy domains in the storage layer of DOW-ECLs. It explains also the effect, where the coercivity of the intermediate layer in a trilayer stack depends on the relative orientation of the (TM subsystem) magnetization of the outer layers (100). For antiparallel orientation, an interface wall is always present and probably shifted across the intermediate layer. For parallel orientation, domains have to be nucleated for the high field branch of the hysteresis loop.

2.3.1.3. Layer Stacks and Protective Layers. The layer stack of an MO disk consists mainly of an MO layer, a dielectric antireflection layer, and a metallic reflection layer (Fig. 14). The thickness of the antireflection layer as well as that of the MO layer have to be properly chosen to obtain a maximum magnetooptical figure-of-merit (FOM). The FOM can be further increased by using a quadrilayer configuration with dielectric layers on both sides of the MO layer. Practical disks use the generalized configuration 50–120-nm dielectric layer, 25–90-nm MO layer, 17–70-nm dielectric layer (for quadrilayer configuration only), and 15–150-nm reflective layer.

The dielectric layers have to fulfill several functions. They must provide a barrier against oxygen and moisture, an antireflection layer for coupling in of the laser light, and heat insulation of the recording layer (in a quadrilayer configuration). Predominantly, AlN and amorphous Si_3N_4 are used as materials for dielectric layers (102), but Ta_2O_5, ZnS, and BaAlSiO sometimes are employed.

2.3.1.4. MO Media Summary. When compared to magnetic recording on hard disks, the advantage of MO data storage is the removability of the disks and the high storage capacity (especially on multiplatter (juke-box) systems) whereas the access times have not yet been reached.

The features of the discussed MO media classes relevant for recording are summarized in Table 3 (35, 68). RE-TM based disks meet all requirements for the first generation of MO recording. Their main deficiency is the need of extra protection layers due to the lack of chemical stability. Pt/Co and garnet disks perform better in this respect, enabling a two-layer stack design. For high performance disks, however, dielectric and metallic

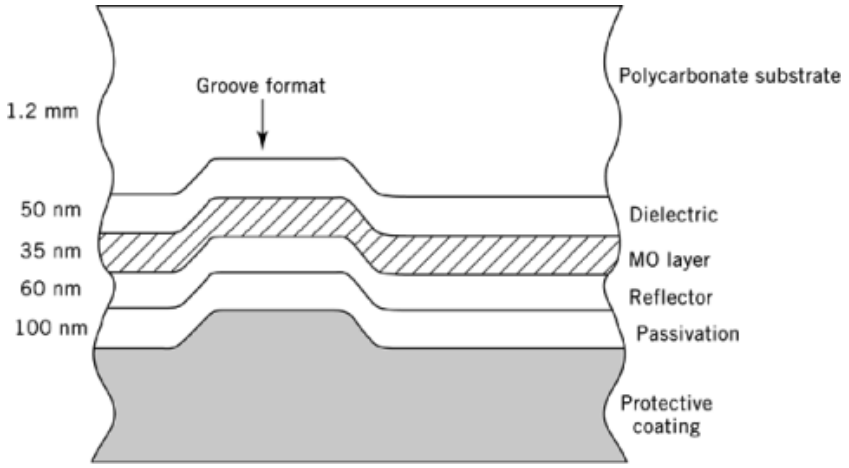

Fig. 14. Cross section of an MO disk (trilayer configuration) (101). Examples of the various layers are dielectric, AlN, Si_3N_4; MO layer, TbFeCo; reflector, Al; passivation, AlN.

layers are always necessary to optimize the optical and thermal properties of the disks. A disadvantage of Pt/Co is their higher magnetization, favoring subdomain formation and stable residual domains after erase, so that the magnetic field during writing and erasing has to be increased. Disadvantages of garnet disks are their high preparation temperature, excluding plastic substrates, and their coarse microstructure, causing noise. Which of these media classes is best suited for recording applications in the range of shorter wavelengths is not yet decided, but due to their fine microstructure and high versatility, RE-TM alloys are still good candidates.

Table 3. Properties of MO Materials

Material[a]	Microstructure	Deposition temperature, °C	H_c,[b] kA/m	θ_K[c]	SNR[d] dB
α-GdTbFe	no grains	RT	> 400	0.3	58
α-TbFeCo	no grains	RT	> 400	0.3–0.4	61
Co-ferrite	0.1–0.5 μm	500	> 250	10/μm	35[e]
Ba-ferrite	40 nm	620	> 100	1/μm	50[f]
Co/Pt	10–30 nm	RT	> 100	0.2	55

[a] Chemical stability of α-GdTbFe and α-TbFeCo is poor; it is good for other materials.
[b] H_c = coercive force. To convert kA/m to kOe, divide by 79.58.
[c] θ_K = Kerr rotations in degrees.
[d] Signal-to-noise ratio measured at conditions: wavelength (λ) = 800 nm, carrier frequency (f) = 1 MHz, linear velocity of the disk (v) = 5 m/s, bandwidth (BW) = 30 kHz, unless otherwise noted.
[e] f = 0.5 MHz, v = 2 m/s, BW unknown.
[f] f = 1.5 MHz, v = 2 m/s, BW unknown.

2.3.2. Phase Change Recording (PC-R)

Erasable and rewritable optical data storage disks in MO technology exhibit in comparison to the widely available magnetic hard disks the possibility for fast disk exchange and in addition a broad insensitivity to dust and magnetic interference. Disadvantageous are their longer access time and a lower data writing rate. As explained earlier, the longer access time is caused by the relatively heavy and thus mechanically inert

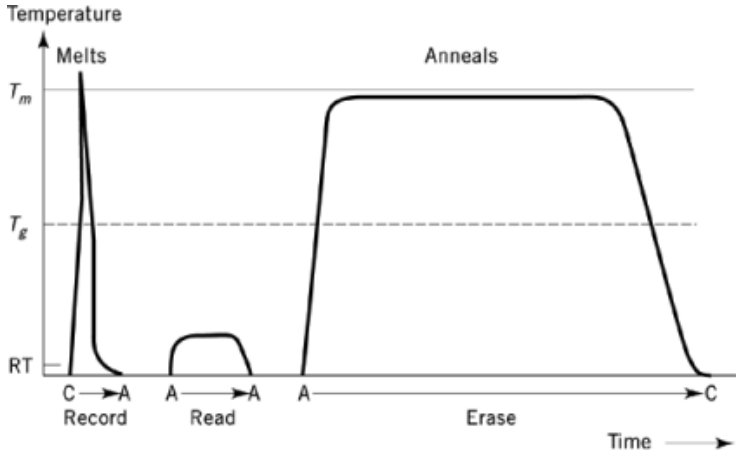

Fig. 15. Time–temperature transformation in a thin-phase change layer during recording/reading/erasing (3, 105). C=Crystalline phase; A=amorphous phase; T_m=melting temperature; T_g=glass−transition temperature; RT=room temperature.

write/read heads of the MO technology, and the lower transfer rate for writing by the absence of a direct overwrite technique. Erasable and rewritable optical data storage disks in PC (phase change) technology unite the advantages of optical storage (high storage density, exchangeable media, robustness) with direct overwrite. On a PC medium the information is stored as amorphous spots in a thin crystalline film. The PC technology is based on fast, reversible transformations between crystalline and amorphous phases of certain alloys. Surveys on that topic can be found (103, 104). Time and temperature plots of write, read, and erase processes in a thin PC layer are shown schematically in Figure 15 (105).

The writing process, that is, the transition crystalline $\longrightarrow$ amorphous, is caused by briefly ($<50-100$ ns) heating up the selected storage area (diameter (φ) ca 0.5–1 μm) by a laser pulse to a temperature above the melting point of the memory layer (Fig. 15, Record), such that the film locally melts. When cooled faster than a critical quench rate ($10^9 - 10^{10}$ K/s), the formation of crystalline nuclei is suppressed and the melted area solidifies into the amorphous (glass-like) state.

The reading of data is performed optically, based on the difference in reflectivity between the well-reflecting crystalline and the opaque and lower reflecting amorphous phase. A low power laser beam is used to avoid crystallization (Fig. 15, Read).

To erase information by the transition amorphous $\longrightarrow$ crystalline, the amorphous phase of the selected area must be crystallized by annealing. This is effected by illumination with a low power laser beam (6–15 mW, compared to 15–50 mW for writing/melting), thus crystallizing the area. This crystallization temperature is above the glass-transition point, but below the melting point of the material concerned (Fig. 15, Erase).

Crystallization processes generally need longer times. The effective dwell time of a particular point of the disk under the laser spot, as determined by the data rate, is about 100 ns. To use this time for heating more effectively, it was proposed first to widen the laser beam elliptically in track direction from 1 to 1–15 μm thus gaining a longer annealing time for crystallization, although this solution would only have allowed erasure of information in blocks (106). Intensive research work has led to alloys that crystallize within about 50 ns when heated by a laser (103).

In PC technology, in contrast to MO technology, the writing is done as direct overwrite, this means that high data transfer rates in the region of 1–10 MByte/s can be reached provided the crystallization time is fast enough, similar to magnetic hard disks and twice as high as for nondirect overwrite MO storage. In addition, since no polarizing optics are needed, the optical read/write head can be built simpler and lighter, which means

it is easier to move. This allows shorter position and access times for a PC system as compared to an MO system.

Special attention has to be given to the long-term stability of the information written in PC technology. Small amorphous areas in a crystalline matrix tend to recrystallize. For that reason, the intensity of the laser beam for reading is held very low, thus allowing a nearly unlimited number of read cycles. In comparison, a high number of write/erase cycles is critical. Besides the selection of suitable, long-term stable PC materials, sometimes the laser energy is adjusted to the number of cycles (107). Based on a crystallization temperature of 320°C and an activation energy of 3 eV, the life span of amorphous domains amounts to about 100 years (3).

Another advantage of PC technology is the planned and partially realized use of multifunction drives for operation of either CD-ROM, WORM, or PC-R disks alternatively in the same disk drive. This is technically feasible, since for reading (in CD-ROM, WORM, PC-R) as well as for writing (WORM, PC-R) similar principles and hardware are used (108). However, the reflectivity change of PC disks (40/70%) is in general lower than the CD-ROM standard (30/70%) requires.

2.3.2.1. Materials for PC Media. Crystalline alloys of elements from the fifth and sixth main group are preferred (3, 103, 109–111). As the first PC materials, tellurium suboxides as well as Te/Se or Te films that had been doped with small amounts of other elements like Ge, As, or Sb to shift the crystallization point to >100°C have been described.

Research has led to alloys which undergo laser-induced crystallization within about 50 ns. This is possible, for example, with TeGe alloys, which also possess the necessary temperature stability up to 180°C and exhibit sufficient reflection (crystalline phase) and transmission characteristics (amorphous phase), respectively. TeGe alloys have not found a practical use because of the formation of depressions in the memory layer typical for them after repeated write/erase cycles (112).

However, typical requirements on PC media and especially the stability/erasability trade off can be illustrated with this system. Pure amorphous Te crystallizes very rapidly (good erasability) but is not stable at room temperature. Alloying a few atomic % of Ge increases the crystallization temperature (better stability) but also raises the minimum crystallization time above the practically available laser dwell time (about 100 ns). This holds equally true in the whole two-phase region, where crystallization implies a phase separation by long-range diffusion. The stoichiometric compound $Te_{0.5}Ge_{0.5}$, however, crystallizes by a polymorphic transformation without long-range diffusion and the necessary crystallization time falls below 100 ns.

More recent are investigations on ternary alloys from InSbTe, GeSbTe (113), TeSeGa, GeTeTi, and InSeSb; in some cases, even quarternary alloys are studied, such as TeGeSnAu. Detailed literature on this topic can be found in References 3,103,109, and 114. GeSbTe is the most studied. The key to achieving high speed is the design of an alloy where the crystallization process involves diffusionsless crystal growth in a system that does not phase segregate. These materials can be crystallized with laser pulses of 30 ns duration and less.

GeSbTe alloys show excellent characteristics for such application, including fast transition times and excellent stability (115). They seem to be best suited for overwriting with linear velocities from 5.6 to 22 m/s. The pseudobinary phase diagram shows that suitable compositions lie on or close to the GeTe–Sb_2Te_3 tie line, eg, $GeSb_2Te_4$, $GeSb_4Te_7$, or the recently commercialized $(GeTe)_2(Sb_2Te_3)_1Sb_{0.5}$ (116). The transition temperature (amorphous $\longrightarrow$ crystalline) T_x increases with increasing GeTe content.

Of importance is the deposition technique for PC layers: suitable PC-materials are applied as thin layers (thickness 20 to 100 nm) predominantly via vapor deposition in vacuum onto proper substrate platters (glass, polycarbonate). To protect the memory active PC layers from oxidation and contamination, they are embedded between two dielectric layers serving as diffusion barriers or heat barriers, respectively (SiO_2, Si_3N_4, AlN, ZnS). A typical layer stack consists, for example, of [ZnS + SiO_2] mixture (180 nm)/GeTeSb (25 nm)/[ZnS + SiO_2] (20 nm)/Al (180 nm) (117). To improve the number of cycles, hard capping layers of MgF_2, CaF_2, or SiO_2 are preferably employed. As thermal barriers between the substrate and memory layer, intermediate layers of Si_3N_4 or AlN are utilized (101). The whole layer stack has to be optimized optically, thermally, and mechanically.

2.3.3. Projected Reversible Optical Recording

In the literature, a multitude of suggestions can be found for possible, reversibly operating optical recording techniques including the materials deemed suitable for this. Common to all these techniques is their failure to develop to commercial use.

2.3.3.1. Reversible Data Storage in Dye Polymer Layers. In the 1970s, attempts were undertaken to reversibly store data in dye-in-polymer films. Corresponding studies were continued in the late 1980s, since pigment–polymer films promise advantages over MO-R and PC-R systems regarding specific performances, eg, signal-to-noise ratio of the reading signal and costs (layer application by spin coating). Three development directions have been pursued: (*1*) reversible generation of depressions, (*2*) reversible bubble generation, and (*3*) reversible deformation.

Reversible Generation of Depressions. This is done in highly dyed or pigmented polymer films by spotwise heating with a laser. Coloring materials, ie, soluble organic dyes or organic pigments with very low solubility in solvents and binders, and with high absorption in the near ir, are used as recording media. The information can be erased by spotwise heating, where the high surface tension of the heated polymer film fills the depression (12, 118). This development does not promise success, however, because of the time-intensive erase process (>100 ms).

Reversible Bubble Generation. In a two-layered pigmented polymeric layer system with ceramic coating, a bubble forms beneath the ceramic coating when heated locally (write process). For erasure, the bubble is closed again by heating the polymer close to its melting point (119). This development is also hampered by extensive erase times (>5 ms).

Reversible Deformation. This is done by spotwise laser illumination of a two-layered composition which consists of a dyed/pigmented thermoplastic and a dyed/pigmented viscoelastic polymer film: on writing, the lower thermoplastic polymer film is thermally expanded using the laser. The emerging deformation is fixed by the viscoelastic film. Erasure is accomplished by heating the thermoplastic film beyond its glass-transition temperature; the resetting forces of the upper viscoelastic layer reverse the deformation (120). With this system, interesting results have been achieved; the erase time is <500 ns, and $>10^3$ write/erase cycles have been reached. For practical use, however, the performance values of MOR or PCR layers should at least be reached approximately.

2.3.3.2. Materials with Reversible Coloring. A dye (or organic pigment) is called photochromic when it is rearranged into an energetically higher isomeric form together with a change of its absorption wavelength under influence of light of wavelength λ_1 (see Chromogenic materials). The reverse reaction can be triggered by absorption of light of wavelength λ_2, thermally, or by both processes simultaneously, where $\lambda_1 < \lambda_2$:

$$A(\lambda_1) \underset{\text{and/or } kT}{\overset{h\nu_1}{\underset{h\nu_2}{\rightleftharpoons}}} A(\lambda_2) \text{ with } \nu_1 > \nu_2$$

The difficulty of such a dye system is that only two variable characteristics (λ_1 and λ_2) have to fulfill three functions (writing, reading, and erasing). If the dye does not absorb, it cannot be switched; if it absorbs, it reacts (the so-called threshold problem). This predicament is circumvented in most cases by either using very low intensity λ_1 or λ_2 light, or using a third wavelength λ_3 for reading at which the dye does not absorb or react which increases hardware complexity.

Another impediment is the demand that both states should be stable in a thermodynamic sense, ie, of the same energy. Practically this cannot be realized; one of the two states will always lie on a slightly higher/lower energy level. For the whole system to remain at least metastable, a sufficiently high activation barrier has to

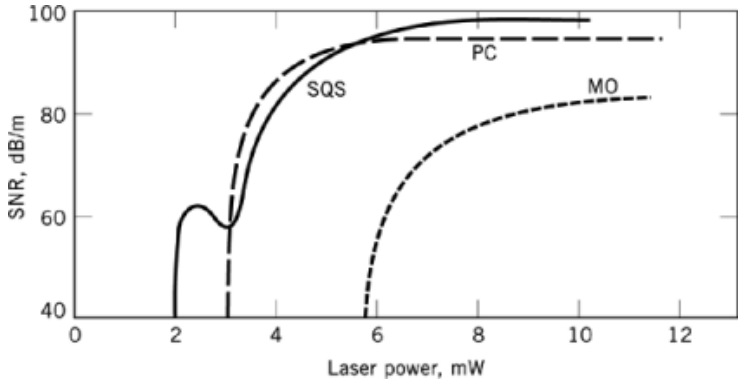

Fig. 16. Maximum achievable signal-to-noise ratio (SNR) on read-out of different writable optical data storage systems as a function of the writing energy (laser power) (121). SQS=Organic dye system (WORM); PC=phase change system (TeSeSb); MO=magnetooptical system (GbTbFe). See text.

lie between the two different energy levels, or the energetically higher level has to be supplied continuously with energy to avoid unwanted shifting of the switching states.

The advantages of dyes are their simple applicability to substrates (spincoating, sublimation, vapor deposition, etc) and their high signal-to-noise ratio on reading, assuming sufficiently high optical contrast (high molecular extinction). Figure 16 shows the maximal achievable SNR for reading data from different storage systems: nonionic squarylium dye (WORM system), GdTbFe-alloy (EOD on MO-R basis), and TeSeSb-alloy (EOD on PC-R basis) (121). The signal from PC and SQS, based on reflectivity changes, is very strong; it is about 10^3 times that of MO media based on RE-TM. In principle, the maximum SNR can therefore be higher for PC and SQS than for MO (Fig. 16). In practice, the obtainable SNR is, however, limited by noise from the written marks (eg, irregularities of their boundaries), so that at present the signal-to-noise ratios are comparable for the two media.

Metallic Alloys with Optically Controllable Coloring. Besides photochromic organic dyes and pigments, metallic alloys with optically switchable coloring, dependent on crystal modification, were the subject of intensive research work in the 1980s. These consist of two or more metals like Al, Cu, Ag, or Zn (10). As an example, the alloy AgZn exhibits a hexagonal crystal structure and silvery color at room temperature. When heated briefly with a laser impulse to 300°C, after cooling down it forms a cubic phase with pink color. Heating to temperatures <300°C restores the initial structure and color (122). A practical application of metallic alloys with optically/thermally controllable coloring, however, is not known.

Photochromic Organic Dyes. Intensive investigations into this category of substances have led to numerous patent applications. Copper–phthalocyanine pigments, organic dyes based on cyanine (Ricoh, Pioneer), naphthochinone (Nippon Denki), and benzothiopyrane (Sony) (123) have been described. They did not lead, however, to any commercial use. Surveys on the possibilities of optical data storage with photochromic dyes can be found (124, 125).

The dyes investigated can be divided into two groups based on the molecular mechanism of their switching. The first types work by electrocyclic opening and cis/trans-isomeric rearrangement. Spiropyrans (126) have found particular interest because of their intensive coloring, which allows application in thin layers and thus fulfills a prerequisite for small pit size and therefore high storage density. Problems are caused, however, by the

spiropyran's lack of chemical stability. A typical representative of this category is the benzospiropyran (127) shown in the following.

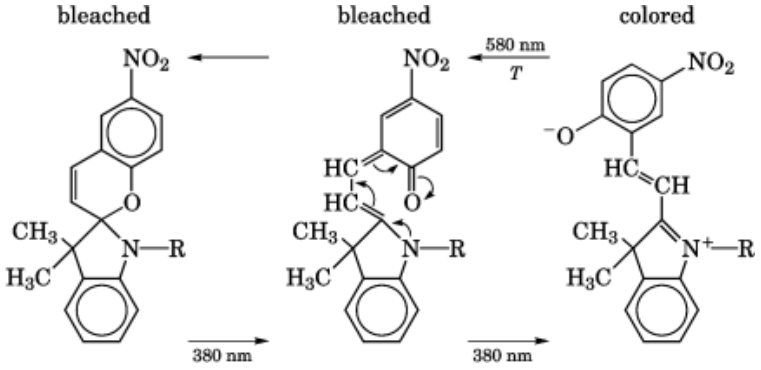

From the colorless state it can be switched with light of short wavelength (λ = 380 nm) via an electrocyclic ring opening and cis/trans rotation of one half of the molecule into a state with violet/purple color. The reverse reaction is effected by visible light (λ = 580 nm). Since the system is metastable, one of the two reaction directions is matched by a rival thermal reaction, the thermoreversion. This progresses, however, in the case of benzospiropyran, at room temperature by a factor of 10^3 slower than the light-induced reaction.

Even though in a solution, all cis/trans isomeric dyes switch fast and almost effortlessly, show a drastic increase in switching time after embedding into polymeric media, and fatigue leading up to a standstill of switching after a few switching cycles. This increase in switching time and debilitation leading to immobility is caused by a steric impediment of free rotation of the dyes by the polymeric matrix (128, 129). For example, benzospiropyrans can be switched in solution in terms of microseconds. After embedding into a polycarbonate matrix, the switching time spontaneously increases by several orders of magnitude. When switched repeatedly, the dye molecule reacts more and more slowly, until it is rendered completely motionless after about 10 switching cycles. This steric impediment is a consequence of relaxation processes of the polymer molecules at and after each switching, since the switching event demands a certain free volume in the polymer matrix for the rotation of the dye molecule. These relaxation processes lead to complete freezing of all motions; that is, a standstill of the switching process in the dye molecule.

The second type of mechanism offers reversible switching without space-consuming transfer processes. These dyes are electrocyclically reacting dyes, where the transition from one form to another form happens by electron shift or proton transfer, without the rearrangement of bulky molecule segments. Fulgides have been proposed for this purpose. Fulgides are bis(methylene) amber acid anhydrides (130), eg, (*E*)-3[1-(2,5-dimethyl-3-furanyl)ethylidene](-4-isopropylidene-2,5 furandione [59000-86-1], $C_{15}H_{16}O_4$, where $R_1 = R_2 = R_3 = CH_3$ and the phenyl ring is replaced by a 2,5-dimethyl furan ring (131). The combination of fulgides with polymers, especially with LC polymers, has led to photochromic recording media for holography and to nondestructive optical read-out systems (132). Dyes from the material class of the fulgides have the disadvantage of generally small molecular extinction (optical contrast differences are too low).

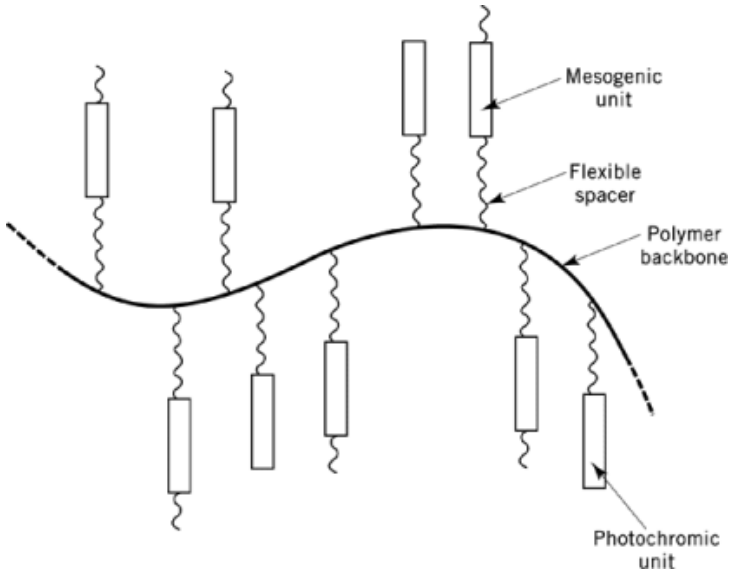

Fig. 17. Schematic structure of an LC side-chain polymer with embedded dyes (134).

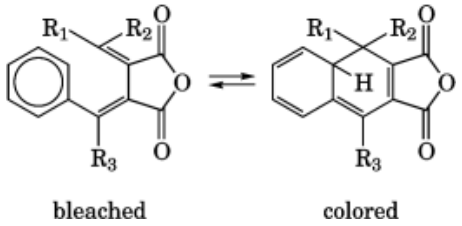

New photochromic dyes with electrocyclic reactions have been proposed on the basis of 1,5-electrocyclization of heterogenous pentadienyl–anions (124). Still newer are investigations into the photocyclization of 2,4,6-tri-isopropylbenzophenones for vinyl polymers in the glassy state (133).

The practical use of photochromic dyes as memory layers in erasable and rewritable data storage disks fails not only because of their physical limitations (lacking sensitivity, insufficient stability, low number of cycles), but also because the diode lasers required for switching in the visible range (wavelength between 450 and 600 nm) and the uv-range (around 350 nm) are not available.

2.3.3.3. LC Side-Chain Polymers with Dyes. All photochromic bistable dyes mentioned have the basic disadvantage that their long wavelength absorbing form is thermally unstable even at room temperature. For that reason, the molecular rearrangements effected by the photoreaction (including the color changes caused by these) are not permanent. To improve long-term stability, storage devices have been developed in which the backbone forms a liquid crystal polymer with mesogens as side chains (LC side-chain polymer). These polymers contain dyes of different nature which are responsible for the switching process. The composition of an LC side-chain copolymer with embedded dyes is schematically displayed in Figure 17 (134). These dyes are, for example, azobenzenes, spiropyrans, or fulgides and the polymer systems are LC polyacrylates and LC polyesters (135), LC polysiloxanes with spiropyran side groups (132, 136), and LC polymers based on methacrylate copolymers with fulgimide side groups (137).

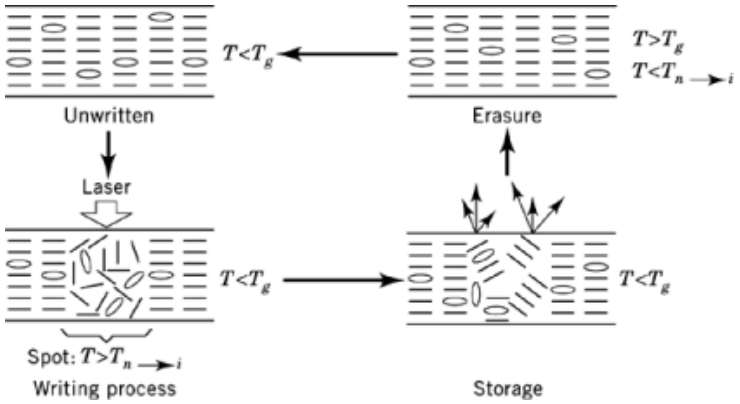

Fig. 18. Single steps of a write/read/erase cycle for an LC side-chain polymer (134). (—), mesogenic group; (⌀), dyestuff. $T_{n\rightarrow i}$ transition temperature nematic⟶isotropic.

In the simplest case the dye-induced storage process is based on a thermally induced phase change between disorder (isotropic melt) and nematic, smectic, or cholesteric ordering of the polymer molecules. Combined with the phase change are corresponding changes in the optical properties. The single steps of a write/read/erase cycle for an LC side-chain polymer with side chains containing dyes is outlined in Figure 18 (134).

In this case, the dye functions only to convert light energy into thermal energy. This process, thermorecording (137, 138), has no technical use due to its large spot diameters caused by the heat transfer of the illuminated spots and its long switching times. In other proposals the phase change is triggered by the spotwise heating of a heat absorbing (generally metallic) substrate of the LC film.

If a dye is used which changes its properties by illumination, eg, its shape like the azobenzene, the phase change temperature can be lowered. The writing process then is nearly isothermal which helps to reduce spot diameters.

This photochemical influence on the shape of systems containing azobenzenes has been investigated. The optically induced transition of azobenzene from the trans into the cis state corresponds to a transition from a mesogenic (stretched) to a nonmesogenic (angled) shape. This causes a disturbance of the liquid crystalline order and leads to a change in birefringence (135). In extreme cases, the order can be destroyed completely; the process then is similar to the thermorecording process depicted in Figure 18.

The photochemically induced phase shift has been investigated (139). The best results were reached when the dye was not mixed physically, but copolymerized into the polymer (140). A big advantage of LC side-chain polymers is the ability to store information at room temperature and thus in the glassy (solid) state, so the information is conserved even when the photochromic dye isomerizes back thermally. Another advantage regarding long-time stability is gained by using photochromic dyes with thermally irreversible photochemistry. This is the case when using special optically reversibly switchable fulgides as mesogenic side groups.

Especially favorable storage effects are achieved by using linearly polarized light instead of unpolarized or circular polarized light. The optical axis of LC polymers in this case is reoriented by up to 90° relative to the polymerization plane of the light beam by cis/trans-isomerization cycles of azobenzene (141). The reorientation process occurs in the solid glassy state and leads to spots with stable phases in the polymer. The resolution is only limited by the wavelength of the writing beam. The induced modulations of structure and optical properties can be erased by global or local heating above the glass temperature. This process has been used for optical storage in homeotropic oriented polymer films (142) and for optical storage in cholesteric systems (143).

The mentioned polymers are in principle suitable for digital data storage, but the practical storage systems introduced up to now are based on polarization holograms. In these systems, use of linearly polarized light

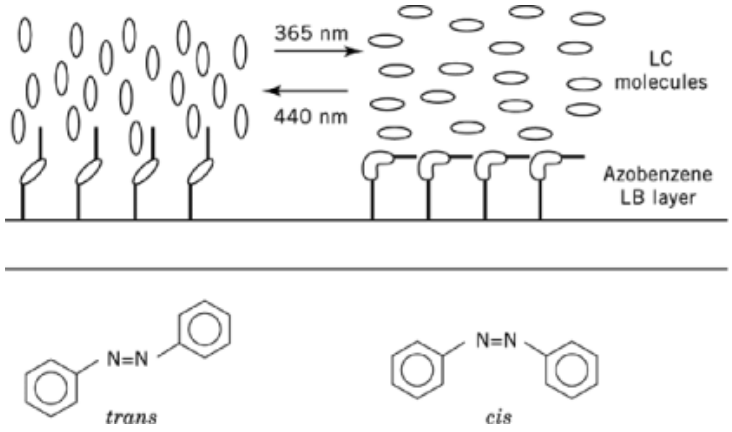

Fig. 19. Reversible data storage by means of a command surface (149, 151–153).

creates birefringence patterns which contain information on the polarization state of the light used for writing (144). It is not only possible to store information on phase and amplitude holographically, as in the common holographic storage media, but also in the polarization state (145) (see Holography).

In Reference 146 three methods for playback of data are presented, which are superior to the usual method based on the contrast in light scattering: readout of dichroism, perpendicular readout mode, and readout of birefringence. Some critical comments also are given about global or selective erasure of data.

Different research groups have examined the special characteristics of LC polymers with photochromic dyes when going to thin films produced by spin coating (147) and ultrathin films produced by the Langmuir-Blodgett (LB) technique (148). Another development variant couples a command surface coated with photochromic dyes with adsorbed, nematically oriented LC polymers (149), sometimes using ultrathin films produced by the LB technique (150). In Figure 19 this principle is demonstrated by a command surface using an LB film of an amphiphilic azobenzene side-chain polymer with a backbone of poly(vinyl alcohol) (151, 152). A photoinduced cis/trans rearrangement of azobenzenes induces a reversible rearrangement of a thick nematic LC polymer attached to the command surface (153).

The application of nonlinear optical recording techniques for reversible optical data storage based on the excitation of photochromic molecules by two-photon processes also has been described (154).

Finally, the use of photoreversible change of the circular dichroism for optical data storage is of interest. This technique offers an advantage over photochromic materials in that the data can be read in a way that does not damage the stored information. These chirooptic data storage devices have been demonstrated with the example of chiral peptides with azobenzene side groups (155).

All LC polymers mentioned herein generally are suitable for digital data storage, especially holographic data storage, because they are thermally stable at room temperature. A disadvantage, however, is the long switching time which is in the order of milliseconds to seconds. For that reason, these polymers currently are not acceptable for fast optical data storage.

2.3.3.4. Biopolymers for Reversible Data Storage. An interesting development for reversible data storage using photochromic materials employs bacteriorhodopsines (BR) optimized by genetic engineering (156, 157). BR is the key protein in the photosynthesis system of the bacterium *Halobacterium halobium*. This bacterium can survive in extreme environments, eg, in concentrated salt solutions or very low temperatures. BR is embedded as a two-dimensional crystalline lattice into the lipid layer of the cell membrane, the so-called purple membrane (PM). A photochrome unit is linked to the polypeptide chain of the BR.

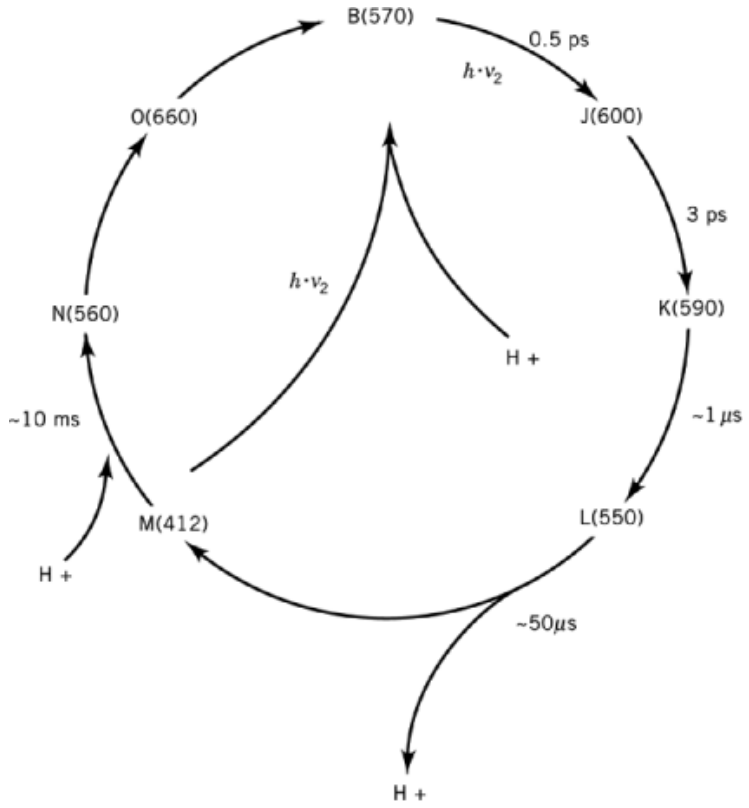

Fig. 20. The photocycle of bacteriorhodopsin with its intermediates including lifetimes and absorption wavelengths in nm in parentheses (158).

Under influence of light, BR acts as a proton pump to generate adenosine triphosphate (ATP). The multistaged photoprocess is depicted in Figure 20 (158). When illuminated with light of 520 nm wavelength, the photochemical reaction B to J is induced; the photochemical transition M to B is triggered by photons of 412 nm wavelength. These photoreactions lead to local changes in optical absorption and index of refraction in the PM film. To read and erase data, preferably in the form of holograms, both photoreactions can be employed: B-type holograms ($B \longrightarrow M$) and M-type holograms ($M \longrightarrow B$).

A technical use of these processes is possible and of high interest because of the special advantages of this system: high quantum yield (0.7), high recording sensitivity ($10^2 - 10^3\ \mu J/cm^2$), good line resolution (>5000 lines/mm), and high number of write/erase cycles ($>10^6$). The shelf life of the written information, however, must be substantially improved. The biological material (so-called wild type) has a duration of the M state of only 10 ms due to thermal relaxation; in contrast, with genetically engineered mutants, durations of over four minutes have been achieved (159, 160). Further development concentrates on breeding of BR mutants with a permanent M state at room temperature.

The purple membrane is harvested semiindustrially from halobacteria mutants which are bred in fermenters. The BR is then embedded into a polymeric matrix of poly(vinyl alcohol) or polyacrylamide. The BR films manufactured in this way are used for different applications, preferably in holography, for example, as a reversible transient data storage system for optical information processing (159). Another example is real-time

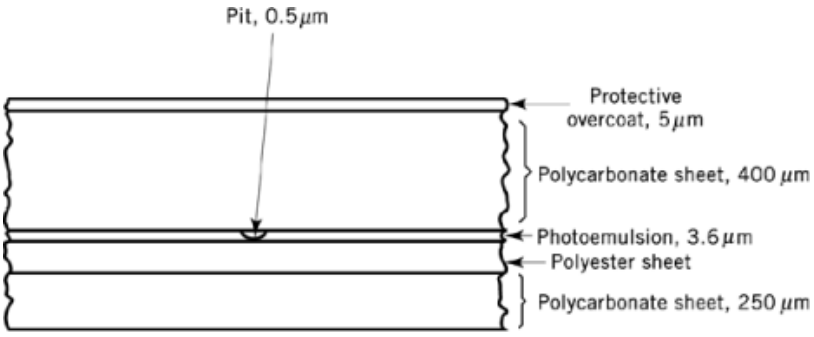

Fig. 21. Principles of optical memory card construction (Laser Card) (163).

interferometry by using the property of BR films to integrate over time (160). BR has been proposed also as a two-photon memory material because of its unusually large two-photon cross section.

Permanent data storage in BR films at room temperature is possible by adding hydroxylamine. In the illuminated areas of the BR film, retinaloxime is irreversibly generated which absorbs at 360 nm. For nondestructive reading, light in the near ir (750 nm) is used (158).

Compared to photographic films, BR is handicapped due to its very low light sensitivity. Also, as a possible material for disk-shaped digital optical information storage, BR does not offer an advantage over established magnetooptical materials in spite of its higher line resolution, because in both cases maximum resolution is determined by the limited wavelength of laser diode light.

2.4. Card-Shaped Optical Data Storage

All commercial magnetic mass storage devices (floppy, hard disk, tape) as well as the optical mass storage devices (CD-ROM, WORM, EOD) require mechanical drives for writing and reading data. Mechanical drives, however, are cost-intensive, bulky, and noisy. They require positioning and access times in the order of milliseconds to seconds, which impedes fast writing and reading of data. Finally, they consume high levels of power, limiting the usable time of portable computers running on batteries.

A possible way of avoiding these disadvantages is offered by solid-state disks, Li-battery-buffered S-RAMs, and EEPROMs. Of special interest are the newly developed flash memories (flash-EPROMs). The last, however, are not freely removable; in addition they are rather expensive and their capacity is limited to around 20 MByte (161). A solution, especially as an alternative to CD-ROM and WORM disks, with the advantage of freely removable media, is offered by optoelectronic memory cards, which can be operated without a mechanical drive. Rather than storing exclusively alphanumeric data like the current magnetic devices or chip-cards, optoelectronic memory cards offer the possibility of storing pictures, graphics, drafts, fingerprints, possibly even sounds, as well as alphanumeric data. Such a credit card-sized storage medium is called optical memory card (OMC).

The composition of an optoelectronic memory card (eg, Laser Card of Drexler Technology Corp.) (162) is outlined in Figure 21 (163). Primary elements are polycarbonate foils with thicknesses of 250 to 400 μm, respectively, that are employed because of their high operating temperature and their good mechanical, optical, and dielectric characteristics. The OMC can be used as a ROM or a WORM media. Both possibilities of information deposition can be used separately or in combination.

An example in the medical field is use as a patient card. Basic data (name, address, date of birth, etc) are written as ROM, but the results of ongoing examinations are written as WORM by the doctor in attendance. For data security, code- and passwords can be used.

One of the benefits of an OMC is its immunity against static electricity and magnetic fields. Its capacity is 4.11 MByte in the version mentioned when used as a ROM, 2.6 MByte for the WORM version.

3. Data Deposition in Three and More Dimensions

3.1. Holographic Information Storage

The techniques described for 2-D storage media use monochromatic laser light for writing and reading. The finite diameter of the laser beam and the optical limit defines the maximum planar storage density using light in the near ir to 10^8 bit/cm^2. Data storage technology aims to concentrate data in the smallest possible space, that is, to achieve maximum spatial storage density. This can be realized by three-dimensional data deposition as a bit oriented format or as an interference pattern (hologram). Therefore, holographic storage techniques attract great interest (164).

The highest information density is achieved by storing information in superimposed volume-phase holograms, so-called thick holograms. The thickness of the storage material must be greater than the wavelength by a factor of >100, so that several thousand holograms can be stored by angle-selective superimposition in the same volume element. With each new hologram the incidence angle is altered by a fraction of a degree.

In a setup for parallel recording and read-out processes in transient holography (158) the superposition of the information-carrying recording beam with a reference beam generates an interference pattern in the recording material, which leads to a spatial distribution of the index of refraction. The information can be read out observing the Bragg condition (see Holography).

Of special interest is 3-D optical data storage by two-photon excitation (165), using two orthogonal laser beams having different wavelengths (166, 167) or, in a simpler scheme, using a single highly focused monochromatic beam (168). Single-beam addressing potentially offers access to extremely high capacity multilayered disk-type storage media.

3.1.1. Materials

For holographic information storage, materials are required which alter their index of refraction locally by spotwise illumination with light. Suitable are photorefractive inorganic crystals, eg, $LiNbO_3$, $BaTiO_3$, $LiTaO_3$, and $Bi_{12}SiO_{20}$. Also suitable are photorefractive ferroelectric polymers like poly(vinylidene fluoride-*co*-trifluorethylene) (PVDF/TFE). Preferably transparent polymers are used which contain approximately 10% of monomeric material (so-called photopolymers, photothermoplasts). These polymers additionally contain different initiators, photoinitiators, and photosensitizers.

When exposed to light, the monomeric material in the photopolymers or photothermoplasts polymerizes, thus locally increasing density and index of refraction. A subsequent fixation process polymerizes the monomer throughout the polymer matrix.

Examples of photothermoplasts include polyacrylates, polyacrylamides, polystyrenes, polycarbonates, and their copolymers (169). An especially well-researched photothermoplast is poly(methyl methacrylate) (PMMA), which is blended with methyl methacrylate (MMA) or styrene as a monomer, and titanium-bis(cyclopentadienyl) as a photoinitiator (170).

Using suitable polymers, the analogously recorded information can be erased blockwise by illumination with light of appropriate wavelength. As an eligible photosensitizer, 2,2-dimethoxy-2-phenylacetophenone has been described (171).

Besides the classical photothermoplasts, LC side-chain polymers with distinct phase changes also are well suited for holographic purposes, and biopolymers from genetically engineered bacteriorhodopsine (BR) have been discussed as a holographic material.

For two-photon memories, a number of media types and reading mechanisms have been used (165). Generally, media comprise two photon-absorbing chromophores dissolved within a solid polymer matrix. Suitable reversible photochromic dyes are, for example, spiropyrans. Although photochromic materials often suffer from photobleaching, as well as from instability leading to self-erasure, new materials and host environments are under development (172). Bacteriorhodopsin (BR) also has been proposed as a two-photon memory material.

All attempts to develop photopolymers or photothermoplasts suitable for fast and reversible recording and read-out of volume-phase holograms, however, have not gained commercial application. The most important characteristics of materials for holographic information recording are listed in Table 4 (158).

Table 4. Materials for Holographic Information Storage[a]

Materials	Spectral range, nm	Resolution, lines/mm	Exposure required, μJ/cm^2	Diffraction efficiency,[b] %	Reusability[c]
silver halide film[d]	400–700	1.000–10.000	10^{-1}–10^2	5–60	
dichromate gelatin[d]	uv–500	$<$ 3.000	10^4	30	
photoresists	uv–650	200–1.000	10^3–10^6	10–85	
photopolymeric materials	300–500	5.000–10.000	10^2–10^4	50	$+10^3$
photothermoplastic materials[d]	400–650	500–1.200	10^1–10^2	10	$+10^1$
magnetooptic materials	700–ir	$>$ 1.000	10^4–10^5	$<$ 0.01	+
photorefractive materials					
$LiNbO_3$	350–500	1.500	10^6	20	+
$Bi_{12}SiO_{20}$	350–550	10.000	10^3	25	+
photochromic materials					
inorganic	300–700	5.000	10^4–10^5	1–2	$+10^3$
organic	400–800	5.000	10^2–10^4	1–2	$+10^3$
biological[e]	400–700	$\geq$ 5.000	10^2–10^5	3	$+10^6$

[a] Ref. 158.
[b] Ratio diffracted/absorbed: irradiated intensity.
[c] Approximate number of times to reuse.
[d] Developing necessary.
[e] Purple membrane from bacteriorhodopsin.

3.2. Photochemical Hole Burning

Aside from holography, photon-gated spectral hole burning (photochemical hole burning (PHB), also named persistent spectral hole burning (PSHB)) is another possibility for achieving multidimensional information storage (173). Besides the three spatial dimensions, the parameters of frequency and electrical field strength can be used to store information.

If dye molecules are embedded into an amorphous matrix, preferably transparent polymers, greatly and inhomogenously broadened spectral lines are observed. This broadening is caused by the energetic interaction of the dye molecules with the locally different environment in the polymer matrix. The ratio of the homogenous initial line width of the dye molecule Γ_h to the inhomogenous line width of the dye in the polymer Γ_i ranges from $1{:}10^3$ to $1{:}10^4$.

If the dye in the polymer is illuminated with frequency stabilized laser light, molecules with absorption frequency identical to the frequency of the laser light are excited. After excitation, the absorption spectrum of the dye-doped polymer exhibits a hole at the location of the laser frequency with the width of the homogenous line of the dye (Fig. 22) (1, 173). This process can be used for building high density data storage systems. The

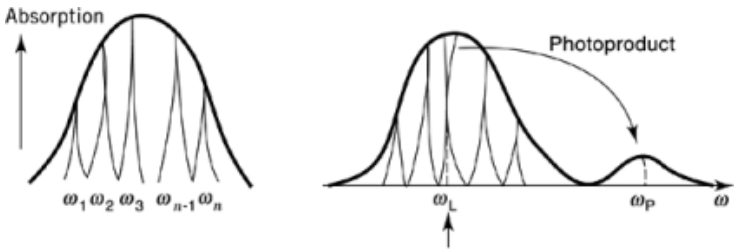

Fig. 22. Photochemical hole burning (PHB) (1, 173) where ω is frequency; ω_L, frequency of the laser; and ω_P, frequency of the photoproduct.

storage density, which is limited in planar data storage to $\leq 10^8$ bit/cm^2 by the frequency of laser light, is increased by frequency selective recording and reading, for example, at $\Gamma_i : \Gamma_h = 10^3 : 1$, to 10^{11} bit/cm^2.

Another possible advantage of the PHB method is its potential multiplexing characteristics; by synchronous recording and read-out, exceptional data transfer rates can be achieved. These high transfer rates are of equal importance in practical data technology as high storage densities.

An interesting development of the PHB technique leads to four-dimensional data storage. By variation of an electric field applied to the sample the spectral profile of the absorption holes can specifically be altered. This adds two more dimensions to the geometrically two-dimensional matrix: frequency of laser light and electrical field strength (174).

A great disadvantage of PHB is the necessity to operate at very low temperatures (<20 K). Therefore, this recording technique currently has no practical significance; but it is subject to intensive research activity (175). One future aspect which may be important, if room temperature materials become available, is the usage of inexpensive semiconductor lasers in the near ir-regime (176).

3.2.1. Materials

Beside inorganic materials (eg, barium chloride/fluoride crystals, doped with 0.05% samarium), transparent thermoplasts are preferred for the PHB technique, eg, poly(methyl methacrylate) (PMMA), polycarbonate, and polybutyral doped with small amounts of suitable organic dyes, organic pigments like phthalocyanines, 9-aminoacridine, 1,4-dihydroxyanthraquinone [81-64-1] (quinizarin) **(1)**, and 2,3-dihydroporphyrin (chlorin) **(2)**.

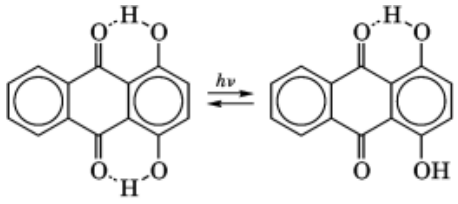

(1)

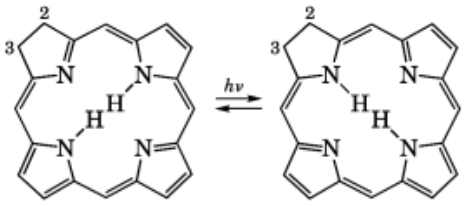

(2)

Current research aims at high efficiency PHB materials with both the high speed recording and high recording density that are required for future memory applications. To achieve this aim, donor–acceptor electron transfer (DA-ET) as the hole formation reaction is adopted (177). Novel PHB materials have been developed in which spectral holes can be burnt on sub- or nanosecond time scales in some D-A combinations (178). The type of hole formation can be controlled and changed between the one-photon type and the photon-gated two-photon type (179).

New PHB materials are composed of Zn-tetrabenzoporphyrin–aromatic cyanide–poly(methyl methacrylate) (180) or of tetraphenylporphyrin derivatives dispersed in polymer matrices such as PMMA and polyethylene (181). A survey of such materials has been given (181).

4. Substrate Materials for Optical Memories

High demands are placed on the substrate material of disk-shaped optical data storage devices regarding the optical, physical, chemical, mechanical, and thermal properties. In addition to these physical parameters, they have to meet special requirements regarding optical purity of the material, processing characteristics, and especially in mass production, economic characteristics (costs, processing). The question of recyclability must also be tackled.

The birefringence of substrate materials for optical data storage devices requires special attention, especially in the case of EOD(MOR) disks. Birefringence has no importance for glass substrates (glass does not exhibit any significant birefringence) and is only a subordinate factor for polymeric protective layers of aluminum substrates because of their reflective read/write technique.

In the case of polymeric substrate materials, high birefringence not only makes exact focusing of the laser beam for reading and writing more difficult, but also effects an unwanted rotation of the plane of polarization during reading, which can severely impair the signal-to-noise ratio, especially using EOD(MOR) disks. In addition, unwanted oscillations in laser intensity are amplified by the reflection of a part of the elliptically polarized light generated by the substrate back into the laser. This feedback, called laser feedback power (LFP), depends on the magnitude of birefringence and the numeric aperture (NA) of the object lens. In a polymeric substrate disk, birefringence is caused by internal stresses in the material (stress birefringence) and/or by preferred orientation of polymer molecules with anisotropic optical polarizability (orientation or rheooptical birefringence). Therefore, polymers with low anisotropy of their molecular optical polarizability are preferred.

The anisotropy of polarizability can be positive (eg, polycarbonate) as well as negative (eg, polystyrene). This offers the possibility of minimizing birefringence by copolymerization or blending of suitable polymers with the right mixture ratio, eg, blends of poly(phenylene ether) (PPE) and polystyrene (PS). The magnitude of birefringence of axial-symmetrically oriented polymers vs their molecule orientation has been described (182).

Lower birefringence can be achieved by concerted efforts during injection molding, meaning an optimized tuning of the temperatures of material and tool injection rate, programming of an injection compression sequence, dynamic pressure, holding pressure, etc (163, 183–185). This care can avoid frozen stresses as well

as a too anisotropic orientation of the polymer molecules. Furthermore, polymers exhibiting a low anisotropy of their molecular optical polarizability are preferably employed.

To efficiently drive the development of improved substrate materials, the limiting values of birefringence have to be known; this is especially true for WORM and EOD(MOR) substrate disks. These limit values were laid down by the ANSI (American National Standard Institute) Technical Standard Committee (186–188). For 5.25 in. WORM disks, the ANSI document X 3 B 11/88-144 recommends a maximum LFP value of 9%; this corresponds to an optical path difference perpendicular to the plane of the disk of not more than 80 nm/mm (double path). For 5.25 in. EOD(MOR) disks, more stringent conditions apply (ANSI-document X 3 B 11/88-049), which also allow calculation of the allowed range.

Depending on the type of memory, further and/or increased demands are imposed. For CD-ROM precise forming of information-containing pits (width 0.6 μm, depth 0.12 μm, length 0.8–3.3 μm) is necessary as are low melt viscosity and easy mold release for high production yields (equals short cycle time). For WORM and EOD(PCR), increased resistance to heat softening (heat distortion temperature (HDT/A) $\geq 150^{\circ}$C) is needed. For EOD(MOR), very low birefringence ($\Delta n < 20$ nm/mm) is required and negligible warp from centrifugal forces at high rotation speeds (tilt angle ≤ 4 mrad at 1.800–3.600 rpm, respectively). There must also be minimal residues of ionic halogen and mold release agents.

With disk diameters above 5.25 in., all parameters, eg, water absorption and thermal expansion, become more critical which aggravates the expansion or warp of disks. If in the future disk rotation speeds have to be increased significantly to boost data transfer rates, higher demands will be placed on warp (tilt angle) and modulus to avoid creeping (ie, irreversible elongation in radial direction). A survey of the requirement profile for the substrate material of optical disks is given in Table 5 (182, 186, 187, 189).

Table 5. Requirements on Substrate Materials for Optical Memories

Properties	Remarks	Nominal value
	Optical properties	
light transmission, %	820 nm	> 90
birefringence, nm/mm	single path	$< 40 (< 20)^a$
optical purity	$\theta \geq 200$ μm	no particles
	Mechanical properties	
thickness, mm		1.20 ± 0.05
thickness, tolerance, μm		± 50
flatness (tilt), degree		± 0.6
surface roughness, nm		< 15
tensile stress, MPa[b]	at yield	> 60
impact strength, kJ/m^2[c]	Izod	no failure
	Thermal properties	
vicat softening temp, $^{\circ}$C	VST/B 50	$> 120 (> 170)^d$
heat defl temp, HDT/A, $^{\circ}$C	(1.80 N/mm^2)[b]	$> 110 (> 150)^d$
	Physical chemical properties	
water absorption, %	immersion	≤ 0.35
water absorption, %	23°C, 50% RH	≤ 0.15
	Processing properties	
melt flow index (MFI), g/10 min	300°C/1.2 kg	> 60
cycle time, s		≤ 7

[a] For EOD(MOR).
[b] To convert MPa (N/mm^2) to psi, multiply by 145.
[c] To convert kJ/m^2 to ftlbf/in^2, divide by 2.10.
[d] For WORM and EOD(PCR).

4.1. Nonpolymeric Substrate Materials

MO disks have to meet particularly high demands in terms of low birefringence; for WORM and EOD(PCR) disks a higher resistance to heat softening is wanted and for all optical storage disks with diameters exceeding 5.25 in. (>130 mm), increased requirements exist regarding smallest warp (thermally or by moisture absorption), distortion, and creep (at very high rotation speeds). These increased demands can be met partially by uv-curable cross-linked polymers, but especially by glass.

4.1.1. Glass

The distinct advantages of glass over thermoplastic polymer materials are high surface quality (surface roughness <3 nm); insensitivity to very high as well as very low temperatures without detrimental expansion/contraction and without warp; no water absorption (water can lead to erosion of sensitive magnetooptical materials and phase change materials, and of the protective layer also); insensitivity to aggressive chemical vapors and liquids; impermeable to gases and vapors; and extremely long shelf life (>25 yrs).

Among the acute disadvantages of glass substrates are high weight; fragility, ie, extremely low fracture toughness (except for special armor glass); and high cost due to intricate, expensive manufacture and the need to apply the formatting layer in a photopolymerization (2P) process in a second, costly production step.

Glass substrates are used commercially for 5.25 in. EOD(MOR) disks only by a few manufacturers (eg, Philips, Hitachi); in contrast, for CD-ROM and WORM memories with disk diameters exceeding 5.25 in. (eg, 12 in. and 14 in.), glass substrates are employed frequently.

4.1.2. Aluminum

Some manufacturers also have WORM disks above 5.25 in. on offer with aluminum as substrate material. For Al the same advantages apply as for glass with the exception of a high coefficient of thermal expansion and lacking resistance to aggressive chemical vapors and liquids.

An advantage of aluminum is the high level of knowledge and the automated production plants stemming from the mass production of Al substrates for magnetic hard disks; these can be widely used for the production of substrate disks for optical data storage.

The limitation to disk constructions with a laser beam reflected at the disk surface is a large drawback, however. This prevents the insensitivity against dust and dirt, which is well known from current optical storage devices with a laser beam reflected after penetration of the transparent substrate. The distance between the disk surface facing the optics and the memory layer naturally has to be much smaller than in common optical disks, where the memory layer is deposited behind a 1.2-mm thick transparent glass or polymer substrate disk.

Another disadvantage of Al substrates is their higher weight compared to polymer substrates, and particularly the significantly higher production costs of the disks themselves.

4.2. Polymeric Substrate Materials

4.2.1. Polycarbonates

Currently, all audio CDs (CD-AD), all CD-ROM, and the biggest fraction of substrate disks for WORM and EOD worldwide are manufactured from a modified bisphenol A–polycarbonate (BPA-PC) **(3)**. In 1991, some 1.3×10^9 compact disks were produced, equivalent to an annual amount of about 35,000 t BPA-PC. WORM and EOD disks are manufactured mainly from BPA-PC for sizes of 5.25 in. and below, and glass for larger form factors (eg, 12 in.), partially also from BPA-PC, and in some cases from aluminum or from cross-linked polymers (epoxy resins) (190).

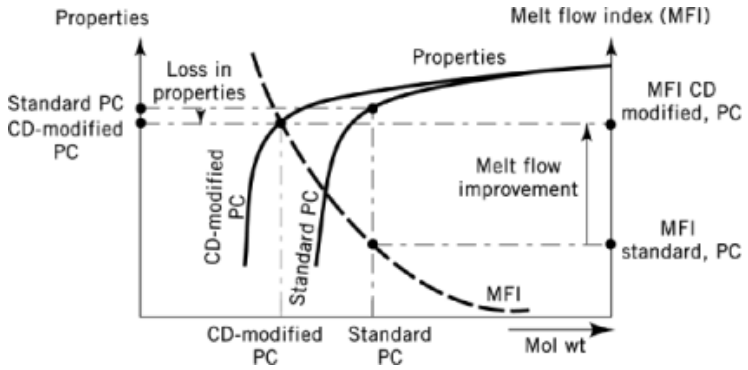

Fig. 23. Correlation between properties (general characteristics), melt flow index (MFI), and mol wt for standard BPA polycarbonate and CD-modified BPA polycarbonate (191, 192).

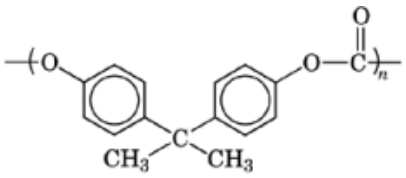

(3)

Modification of BPA-PC for adaptation to the conditions of production of CD and CD-ROM disks, and of substrate disks for WORM and EOD was necessary. BPA-PC standard qualities for extrusion and injection molding have, depending on molecular weight, melt flow indexes (MFI), (according to ISO 1130/ASTM 1238 in g/10 min at 300°C/1.2 kg, between less than 3 g/10 min (viscous types) up to 17 g/10 min. For CDs and optical data storage disks, however, MFI values exceeding 30 g/10 min, and for exceptionally short cycle times (5–7 s) even $\geq 60\ g/10min$ are demanded at an injection mass temperature of 300°C (see Table 5).

An increase in MFI can be gained by lowering the molecular weight (MFI line in Fig. 23), but this has to be weighed against a steep decrease in general characteristics, eg, resistance to heat softening and impact resistance (Standard PC line in Fig. 23). Possibilities therefore had to be found to shift the characteristics line to lower molecular weights. This could be achieved by exchanging the usual phenolic end groups by *p*-alkylphenols with branched alkyl groups. For the so-called CD qualities, the MFI could be increased to values around 66 g/10 min by lowering the molecular weight from about 30,000 to about 18,000, this without a significant loss in characteristics (CD-modified PC line in Fig. 23) (191, 192).

At the same time, a decrease in orientation- and stress-birefringence for the modified BPA-PC could be achieved by optimizing the processing conditions (184,187,189,190,193); this lowers birefringence below $20\ nm/mm$ (single path) for injection-printed injection molded CDs and substrate disks (Fig. 24) (191). The typical characteristics of a modified BPA-PC especially developed for CD production are listed in Table 6 (187, 193).

Although CD-modified BPA polycarbonate can be employed without problems for CD-DA and CD-ROM, the use as a substrate material for EOD(MOR) requires an optimum selection and meticulous adherence to production conditions to achieve the required birefringence values of less than $20\ nm/mm$ (184, 193).

For substrates of WORM and EOD(PCR) disks the industry in the future wants polymers that have a markedly improved resistance to heat softening compared to BPA-PC and, if possible, a lower water absorption and lower birefringence, but otherwise maintain the good characteristics in toughness, production, and cost

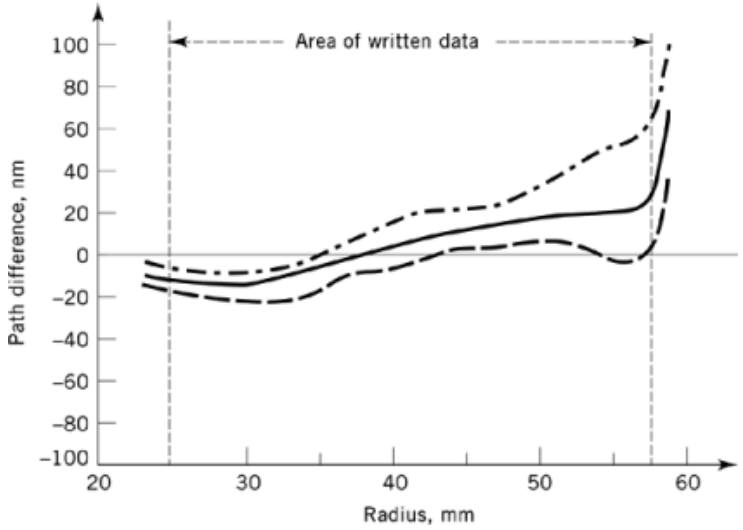

Fig. 24. Birefringence (path difference) of a compact disk, made from CD-modified BPA polycarbonate (191). (), max value; (), min value; (—), mean value.

Table 6. Characteristic Properties of CD-Modified BPA Polycarbonate[a]

Properties	Standards	Value
Optical properties		
refractive index	ASTM D542	1.583
light transmission (λ = 800 nm); 3.2 mm, %	ASTM D1003	92
birefringence (single path), nm/mm		<40[b]
Thermal/mechanical properties		
vicat softening temperature VST/B 120, °C	ASTM D1525	141
heat deflection temperature HDT/A, B, °C	ASTM D648	120/134
tensile stress at yield, MPa[c]	ASTM D636	62
elongation at break, %	ASTM D638	>50
impact strength (notched Izod; 3.2 mm), J/m[d]	ASTM D256	410
Physical/chemical properties		
water absorption (immersion), %	ASTM D570	≤0.35
water absorption (at 23°C, 50% rh), %	ASTM D570	<0.15
Rheological properties		
melt flow index (300°C/1.2 kg), g/10 min	ASTM D1238	70
Processing properties		
cycle time, s		7[e]

[a]Makrolon CD 2005, Bayer AG (Germany) and Mobay Corp. (United States) (193).
[b]With optimal processing: <20 nm/mm.
[c]To convert MPa to psi, multiply by 145.
[d]To convert J/m to ftlbf/in., divide by 53.38.
[e]With optimal processing: < 5 s.

(194). This goal is being approached in different ways: further modification of BPA-PC, newly developed polymers, improvement of the processing characteristics of uv-curable cross-linked polymers, and development of special copolymers and polymer blends, eg, TMBPA-PC/SAN and PPE/PS.

4.2.2. Polycarbonates with Improved Heat Resistance

The high optical anisotropy of BPA-PC is mainly caused by the strong polarizability of the aromatic rings in the backbone. This inherent high birefringence of PC can be reduced by the installation of groups with high birefringence (eg, phenyl groups) in lateral side groups (195, 196).

The birefringence for phenyl-substituted PC **(4)** (T_g = 176°C) is reduced to about 50%, for benzyl substituted PC **(5)** (T_g = 138°C) to about 25%, and for four-ring bisphenol PC **(6)** to 8% of the value for BPA-PC (183,190,195,197,198) on condition of an optimum conformation of the phenyls in the side groups perpendicular to the aromatic rings in the backbone. In reality, however, these low birefringence values are not achieved, because the optimum conformation of the phenyl rings cannot be achieved in injection-stamped disks.

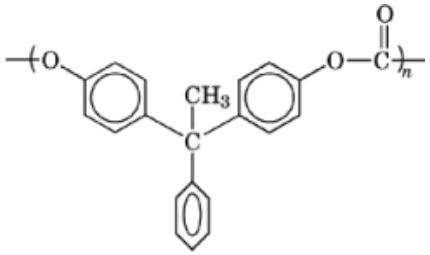

(4)

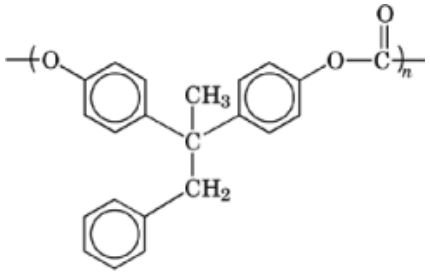

(5)

Regarding the glass-transition temperature, only the four-ring bisphenol-PC **(6)** exhibits a remarkable increase of T_g (220°C) over BPA-PC, but the high brittleness prohibits its use in practical applications (195, 196).

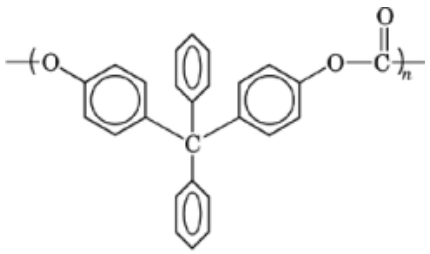

(6)

Numerous attempts have been made to reach improved products by installing phenyl side groups on the aromatic rings of the backbone; for this, sometimes the isopropylidene group has been partially or wholly substituted. The corresponding products exhibit a greatly reduced birefringence, but their resistance to heat softening leaves something to be desired (199). The same holds true for polycarbonates with *t*-butyl and isopropyl substituents on the rings of the backbone (200).

Another path has been followed by completely changing the isopropylidene group. Replacement by a side-based cyclohexyl ring by itself raises the glass-transition temperature markedly (179°C) **(7)** (201); the additional lowering of birefringence by *t*-butyl or phenyl substituent groups on the aromatic rings of the backbone, however, results in overall reduction of T_g, 152°C for *t*-butyl; 161°C for phenyl (202).

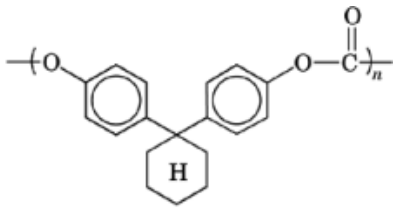

(7)

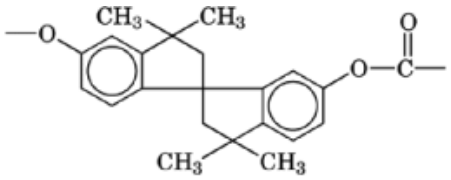

(8)

A decisive breakthrough to a T_g range above 230°C was achieved with a polycarbonate based on spirobisindan (SBI-PC, **(8)**) (203) or 3,3,5-trimethylcyclohexane (TMC-PC, **(7)** wherein the cyclohexane ring bears three methyl groups) (204).

The nearly symmetrical composition of SBI-PC (T_g = 230°C) makes birefringence disappear in homopolymers, but the material becomes very brittle due to the blocking of the free rotation of the aromatic rings, which puts its technical application in question. Only a copolymerization with 80 wt % BPA-PC reaches sufficient levels of impact resistance; but T_g is lowered to 170°C and birefringence increases to 80% of that of BPA-PC (195, 196). In contrast, TMC-PC as a homopolymer already has sufficient impact resistance at a T_g of 238°C and a birefringence of 83% of that of BPA-PC (195, 205) (Table 7).

4.2.2.1. Copolymers and Blends of PC. Numerous co- and terpolymers as well as polymer blends of BPA-PC have been developed and their suitability as substrate materials for optical data storage media has been tested (Table 8) (195). From these products, three lines of development have been chosen for closer examination.

Copolymers and Blends of BPA-PC and Modified PS. Theoretically, a blend or copolymer of 60 parts BPA-PC (positively birefringent) and 40 parts PS (negatively birefringent) should yield a product free of birefringence (Fig. 25) (207). In spite of modifications to PC to improve the compatibility, no blend could be produced which would be optically isotropic and thus suitable as a substrate material. The same holds true for PC/PS-copolymers (208) in which PC : PS = 77 : 33.

Table 7. Properties of TMC-Polycarbonate and its Copolymers with BPA-Polycarbonate[a]

	BPA-PC:TMC-PC				
Property	100:0	80:20	65:35	45:55	0:100
glass transition temperature, T_g, °C	149	174	187	205	238
heat resistance HDT-B (0.45 N/mm^2),[b] °C	138	163	174	195	223[c]
impact strength (ISO 180),[d] kJ/m^2[e]	not broken	not broken	not broken	not broken	[f]
notched impact strength, kJ/m^2[e]	45	14	8	<8	<5
melt viscosity (at 360°C and shear rate = 1000 s^{-1}), Pa·s[g]	120	170	220	280	380
max birefringence $\Delta n \times 10^3$	2.06	1.99[c]	1.93[c]	1.86[c]	1.70

[a] Ref. 206.
[b] To convert N/mm^2 to psi, multiply by 145.
[c] Interpolated data.
[d] nb = not broken.
[e] To convert kJ/m^2 to ftlbf/in^2, divide by 2.10.
[f] From 10 measurements of 0:10, eight are nb and two ≥ 150 kJ/m^2.
[g] To convert Pa·s to P, multiply by 10.

Table 8. Substrate Materials for Optical Data Storage

Substrate material	Manufacturer
Copolymers	
copolymer of PC and styrene (24:76)	Idemitsu
graft copolymer of PC and styrene	Mitsubishi
copolymer of PC with *o,o*'-biphenyl units, T_g = 160°C	Toray
copolymer of PC with dihydroxytricyclodecane units, HDT = 135°C	Tosoh
copolymer of PC and spirobisindane–PC (SBI-PC)	General Electric
copolymer of PC and trimethylcyclohexane–PC (TMC-PC)	Bayer AG
Blends	
PC with modified polystyrene (60:40)	Sumitomo
PC with MMA–styrene copolymer (LCST[a] =~ 240°C)	Mitsubishi
PC with SMA copolymer	Nippon Steel
PC with dimethyl BPA-PC	Bayer AG
PC with four-ring bisphenol-PC	Bayer AG
PC with trimethylcyclohexane–PC (TMC-PC)	Bayer AG
PC-cocondensates (BPA-PC, benzyl-substituted PC, four-ring bisphenol-PC, PC with lateral phenyl side groups on the aromatic rings)	Bayer AG
TMBPA-PC with polystyrene (62:38, LCST[a] =~ 240°C)	Philips
TMBPA-PC with modified PS	Tosoh
TMBPA-PC with modified SAN	Bayer AG

[a] LCST = lower critical solution temperature.

Blends of Tetramethylbisphenol A-PC (TMBPA-PC) with Modified PS or Styrene-Acrylonitrile(SAN) Copolymer. By installing halogen atoms on the aromatic rings of the PC-backbone, not only the resistance to heat softening can be increased (eg, TMBPA-PC: T_g = 203°C) (209), but also the compatibility with olefins. Optically homogenous blends have been described (210) of TMBPA-PC (positively birefringent) with modified PS or modified SAN (both negatively birefringent) (see Table 8); due to their low birefringence and increased resistance to heat softening these products have been recommended as substrate materials for magnetooptical data storage (197, 198).

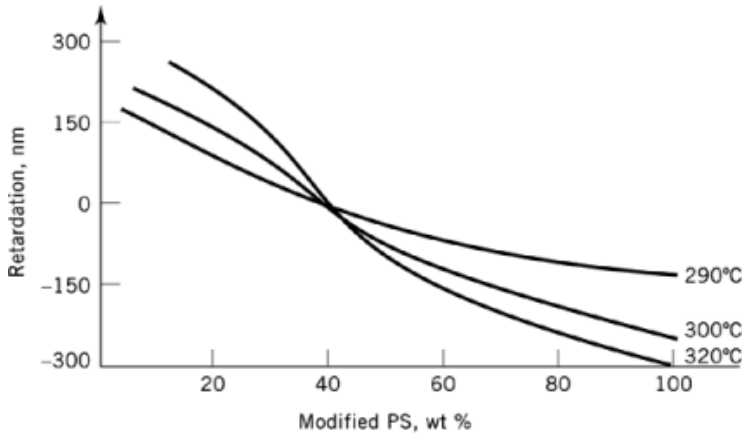

Fig. 25. Influence of blend composition on birefringence (207). Blend is PC and modified PS. Temperatures noted are molding temperatures.

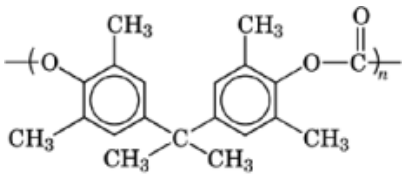

(**9**)

Copolymers of BPA-PC with TMC-PC. These copolymers (206) (APEC-HT, Bayer AG, Leverkusen, Germany) have high resistance to heat softening, sufficient impact resistance, lower birefringence than BPA-PC, and low melt viscosity for easy processing. The most important data of selected copolymers was shown in Table 7 (195, 206). These values reveal the material's fitness as a basis material for optical data storage disks especially when resistance to heat softening is required which is markedly higher than that of BPA-PC.

4.2.3. Poly(methyl methacrylate)

PMMA offers distinct advantages over BPA-PC with respect to significantly lower birefringence, higher modulus, and lower costs, but has not been successful as a material for audio CDs and CD-ROM as well as a substrate material for WORM and EOD disks because of its high water absorption (which makes it prone to warp) and its unsuitability for metallizing, and less so because of its low resistance to heat softening. Only 12 in. video disks are manufactured from PMMA by injection molding or the 2P process (photopolymerization process), because the glued sandwich arrangement in this product prevents warp due to high water absorption.

In the literature (182, 189, 211) can be found numerous studies which tried to alleviate these disadvantages by modification, copolymerization, or blending with proper partners: MMA/CHMA copolymers (methyl methacrylate/cyclohexyl methacrylate) have a lower water absorption than pure PMMA but at the price of a reduction in strength (182, 189). MMA/St copolymers (methyl methacrylate/styrene) also show lower water absorption but have a higher birefringence (182). For PMMA–PVC blends (212) and PMMA–PVDF blends (213) (PVC = poly(vinyl chloride), PVDF = poly(vinylidene fluoride)) in the right blend mixture, birefringence is indeed canceled out, but the other properties (eg, resistance to heat softening) do not meet the requirements.

More recently, test products were created of a blend of PMMA with a phenyl-substituted methacrylate; these products have a glass-transition temperature of around 125°C, a significantly reduced water absorption compared to pure PMMA of about 0.32%, but also a higher birefringence (a stress-optic coefficient of 5.2×10^{-11}, compared with 0.3×10^{-11} for PMMA and 6.8×10^{-11} for BPA-PC).

4.2.4. Cyclic Polyolefins (CPO) and Cycloolefin Copolymers (COC)

Japanese and European companies are developing amorphous cyclic polyolefins as substrate materials for optical data storage (213–217). The materials are based on dicyclopentadiene and/or tetracyclododecene **(10)**, where R = H, alkyl, or $COOCH_3$. Products are formed by Ziegler-Natta polymerization with addition of ethylene or propylene **(11)** or so-called metathesis polymerization and hydrogenation **(12)**, (101, 216). These products may still contain about 10% of the dicyclic structure (216).

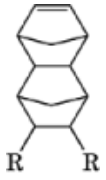

(10)

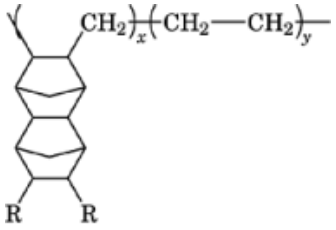

(11)

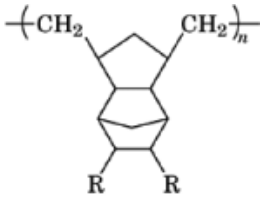

(12)

The production of CPO is based on relatively inexpensive cyclic substances; these must be derivatized, however, to meet the requirements of resistance to heat softening and suitability for metallization. Metathesis polymerization is problem-prone, since relatively large amounts of catalyst (WCl_6, $C_2H_5AlCl_2$) must be removed by solvent extraction (216). In the process, the price of CPO, at small batches, is several times higher than that of BPA-PC.

The principal advantages of CPO over the current substrate materials based on BPA-PC are very low water absorption (depending on type less than 0.1%), resistance to polar solvents and to acids and bases, low birefringence (comparable to that of PMMA), and short vacuum time (for sputtering ferrimagnetic layers).

Disadvantages include high proneness to warp, low impact resistance, significantly higher melt viscosity (longer cycle time in disk production), unsatisfactory metallizability, and high expense.

Table 9 compares the most important properties of substrate materials based on BPA-PC, PMMA, and CPO (three different products) (216, 217). The future will prove if the current disadvantages of CPO against BPA-PC regarding warp, processibility (melt viscosity), and especially cost can be alleviated. Cyclic polyolefins (CPO) and, especially cycloolefin copolymers (COC) (218) and blends of cycloolefin copolymers with suitable engineering plastics have the potential to be interesting materials for substrate disks for optical data storage.

Table 9. Comparison of Characteristic Properties of Substrate Materials

Properties	BPA-PC[a]	PMMA[b]	CPO[c]	CPO[c]	CPO[c]
light transmission, %	>90	>90	>90	>90	92
birefringence, nm/mm	<40	<20	<25	<20	<20
glass-transition temperature, °C	145	105	140	171	150
tensile stress at yield, MPa[d]	62	73	64	42	59
elongation at break, %	>50	5	10	16	3
impact strength, notched kJ/m^2[e]	20–30	2	4	3	
water absorption, (100% rh), %	<0.35	2.1	<0.01	0.2	0.01
melt flow index (280°C), g/10 min	57		15		
vacuumizing time,[f] min	78	200	14		

[a] CD-modified BPA-polycarbonate (CD 2005, Bayer AG).
[b] Poly(methyl methacrylate).
[c] Cyclopolyolefins.
[d] To convert MPa to psi, multiply by 145.
[e] To convert kJ/m^2 to ftlbf/in.^{2}, divide by 2.10.
[f] Mitsui method

4.2.5. Cross-Linked Polymers

In the 1980s, not only glass and BPA-PC but also uv-curable cross-linked polymers, eg, epoxy resins, were used as substrate material for optical mass storage disks with large diameters (12 in., 14 in.) (219). The epoxy resins consisted of compounds containing one or several highly reactive epoxy or hydroxyl groups. The common epoxy resins (EP) mainly are reaction products of bisphenol A and epichlorohydrin:

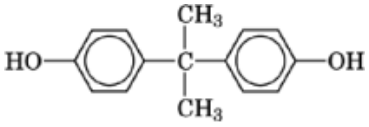

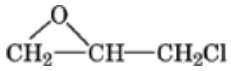

The resulting bisepoxy compounds are cross-linked cold with polyamines, if necessary with added accelerators. A hot cure can either be accomplished with amines or anhydrides (eg, phthalic acid anhydride). If suitable initiators are present, EP systems can also be cross-linked by radiation.

Special, uv-curable epoxy resins (qv) for substrate disks for optical data storage (Sumitomo Bakelite, Toshiba) excel by means of their very low birefringence (<5 nm/mm) and high Young's modulus. Resistance to heat softening and water absorption are similar to BPA-PC, but impact resistance is as low as that of PMMA.

The decisive disadvantage for industrial mass production of substrate disks is the extremely long curing time (eg, 5 h at 100°C); thus efforts to reduce curing time have been numerous. It is possible to produce substrate disks with up to 30-cm diameter by using uv-curing reaction resins based on unsaturated carbon acid esters and other vinyl compounds. The cycle times are as low as 15 to 100 s when an additional post-cure, as necessary for all cross-linked polymers with high T_g, ranging from 1 to 5 h at 60 to 100°C, is applied (220).

Table 10 compares the values of different experimental uv-curable cross-linked polymers with those of BPA-PC for the most important properties of substrate materials (220). In spite of this remarkable progress in the development of fast curing cross-linked polymers, BPA-PC and, to a small extent, glass are still the materials of choice for substrates for optical data storage.

Table 10. Comparison of Characteristic Properties of CD-Modified BPA-Polycarbonate with UV-Curing Duromer

Properties	BPA-polycarbonate[a]	UV-curing duromers[b]
refractive index, n^{D}mn	1583	1.55–1.58
birefringencec[c], nm/mm		
M_1	<40	0–10
M_2	500–800	60–100
light transmission, %	90–92	90–92
glass-transition temperature, °C	145	120–200
water absorption (100% rh), %	0.35	0.36–0.13
coefficient of linear thermal expansion, 10^{-6}/K	51–71	60–75
tensile modulus, N/mm^2[d]	2300	3000–4000
impact strength, kJ/m^2[e]	not failure	20–4
release time/setting time, s	7	100–15 (uv)[f]

[a] CD-modified BPA-polycarbonate (CD 2005, Bayer AG (Germany) and Mobay Corp. (United States)).
[b] Duromers (cross-linked polymers) based on highly reactive resins with short setting times.
[c] Laboratory conditions: M_1 (direction perpendicular to disk plane) ≤ 20 nm/mm; M_2 (parallel to plane) ≤ 500 nm/mm.
[d] To convert N/mm^2 (MPa) to psi, multiply by 145.
[e] To convert kJ/m^2 to ftlbf/in.^{2}, divide by 2.10.
[f] Additional (60–120°C) ca 1–5 h.

4.2.6. Other Polymers

Besides polycarbonates, poly(methyl methacrylate)s, cyclic polyolefins, and uv-curable cross-linked polymers, a host of other polymers have been examined for their suitability as substrate materials for optical data storage, preferably compact disks, in the last years. These polymers have not gained commercial importance: polystyrene (PS), poly(vinyl chloride) (PVC), cellulose acetobutyrate (CAB), bis(diallylpolycarbonate) (BDPC), poly(ethylene terephthalate) (PET), styrene–acrylonitrile copolymers (SAN), poly(vinyl acetate) (PVAC), and for substrates with high resistance to heat softening, polysulfones (PSU) and polyimides (PI).

Reduction or even complete compensation of birefringence by mixing polymers with positive birefringence (PC, PVC, PETP, PPE, PVDF, etc) with polymers with negative birefringence (PMMA, PS, PAN, etc) has been the consistent strategy.

Newer developments involve poly(4-methyl-1-pentene) (TPX), PS or PPE blends, and block copolymers.

The TPX experimental product of Mitsubishi Petrochemical Ind. (221) is an amorphous, transparent polyolefin with very low water absorption (0.01%) and a glass-transition temperature comparable to that of BPA-PC (ca 150°C). Birefringence (<20 nm/mm), flexural modulus, and elongation at break are on the same level as PMMA (221). The vacuum time, the time in minutes to reach a pressure of 0.13 mPa (10^{-6} torr), is similarly short like that of cyclic polyolefins. Typical values of TPX are listed in Table 11. A commercial application of TPX is not known as of this writing.

Experimental products with a mass ratio of polystyrene to poly(phenylene ether) (PS : PPE = 65 : 35) exhibit glass-transition temperatures of 136°C and water absorption of 0.1% (according to other measurements,

Table 11. Comparison of Different Substrate Materialsa

Property	Test method	CD-modified BPA-PC	TMC/BPA-PCb
density, g/cm^3	ASTM D792	1.2	1.2
light transmission, %	ASTM D1003	> 90	90
refractive index	ASTM D542	1.583	1.565
Abbe number, $\frac{n-1}{n_{bl}-n_{red}}$		30	~ 30
birefringence, nm/mm	single path	< 40	< 35
glass-transition temperature, °C	DSC method	145	205
heat defl temperature, HDT/A, °C	ASTM D648	129	179/197f
bending modulus, MPag	ASTM D720	2.400	2.200
elongation, at break, %	ASTM D636	> 50	50
flatness (tilt), mrad		< 5	< 5
impact strength (Izod), kJ/m^{2}i	ISO 180/1C	not broken h	not brokenh
notched impact strength (Izod), kJ/m^{2}i	ISO 180/1A	20–30	5–8
melt flow index, g/10 min (280°C)	ASTM D1238	57	~ 30
vacuumizing time, min (1.3 mPaj)	Mitsui method	78	78
water absorption, % 23°C, 50% rh	ASTM D570	0.15	0.15
water permeation, g/m^2 24 h		1.53	1.53
processing ease		+	+

[a] Ultraviolet-curing cross-linked polymer.
[b] Cyclopolyolefin (two different products).
[c] Poly(4-methyl-1-pentene).

0.4%) together with excellent transparency (>90% light transmission); birefringence in cast test samples (without orientation of molecules due to injection molding) is completely compensated (222, 223). Typical values of this blend are also listed in Table 11. Interestingly, blend composition for no birefringence depends strongly on the molecular weight of the individual components (223). In injection molded test samples, a strong dependence of birefringence on the processing conditions could be seen. This product also is still waiting for a commercial application. Calculations of Sumitomo Chemicals show that only an annual production upward of 1000 to 2000 t (corresponding to about 30 to 60×10^6 substrate disks of 5.25 in. dia) would be economical (224).

It has been reported that block copolymers with appropriately chosen partners and mixing ratios yield materials suitable for use in substrate disks for optical data storage. An example is polyarylate–polystyrene block copolymer with a PS content between 40 and 60% (225).

5. Comparison of Substrate Materials

For CD-DA (CD-digital audio) and CD-ROM including all variants, a CD-modified BPA-PC is used exclusively. BPA-PC is stipulated in the specifications for CD-DA.

WORM disks with diameters of 130 mm (5.25 in.) and 200 mm (8 in.) are manufactured almost exclusively from modified BPA-PC, including Kodak's Photo-CD. Glass is used predominantly only for WORM disks with 300 mm (12 in.) diameter.

For EOD disks with 86 mm (3.5 in.) diameter and for Sony's Mini-Disk (67 mm diameter), modified BPA-PC is used exclusively; for EOD disks with 130 mm diameter, modified BPA-PC (mainly) as well as glass (eg, Philips, Hitachi) are used.

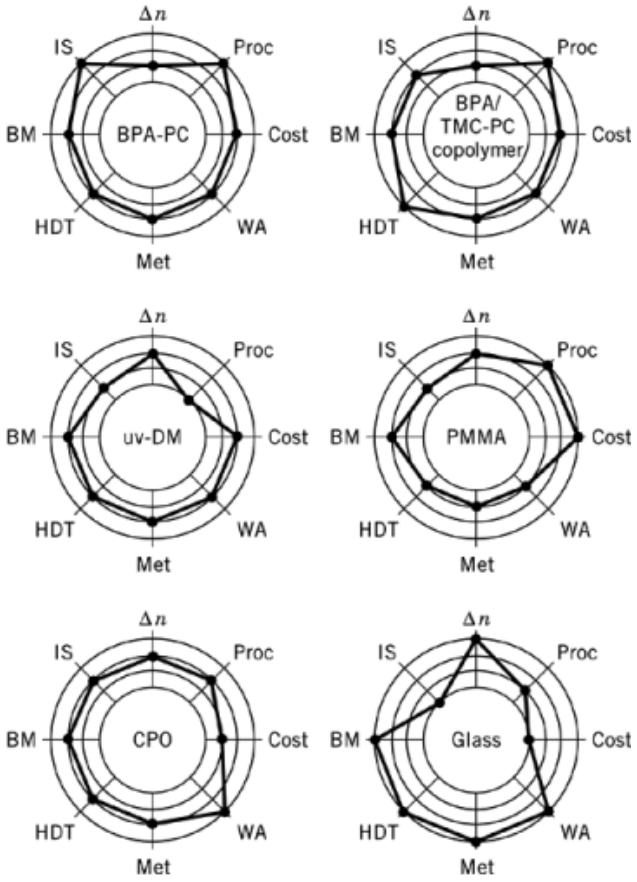

Fig. 26. Qualitative comparison of substrate materials for optical disks (187): Δn=birefringence; IS=impact strength; BM=bending modulus; HDT=heat distortion temperature; Met=metallizability; WA=water absorption; Proc=processibility. The materials are bisphenol A–polycarbonate (BPA-PC), copolymer (20:80) of BPA-PC and trimethylcyclohexane–polycarbonate (TMC-PC), poly(methyl methacrylate) (PMMA), uv-curable cross-linked polymer (uv-DM), cyclic polyolefins (CPO), and, for comparison, glass.

In spite of the decision of commercial suppliers of digital optical storage disks, it is of interest to compare the most important properties of glass and polymers and rate them according to their characteristics relevant to optical storage disks. For a direct visual comparison, Figure 26 depicts the most important properties relevant to data storage in spider charts. The innermost circle symbolizes the most unfavorable case of each property and the outermost circle the most favorable case (187). Table 11 presents the numeric values available thus far; if varying numbers exist, a qualitative assessment was made (according to Ref. 216).

Of practical interest are detailed studies to influence the magnetooptical properties of RE-TM materials by the substrate material and the substrate adhesion of RE-TM layers by the selected deposition technique (226). Accordingly, measurements have been performed on glass, BPA-polycarbonate, and poly(ethylene terephthalate) (as a flexible substrate).

6. Future Developments

The question as to whether and to what extent and in what area optical mass storage would replace magnetic systems (disk, tape) was controversially being discussed in the 1980s. In spite of all predictions of an imminent substitution, as of late 1994 magnetic hard disks still are the system of choice for computer-dedicated mass storage due to their speed (access time, transfer rate), physical size, and energy consumption; this is especially true when memory-intensive applications are run which use the hard disk as virtual memory.

There is no competitive situation for data storage disks with embossed information (CD-ROM) and recordable/nonerasable disks (WORM); no counterpart to CD-ROM and WORM exists among magnetic memories. EOD drives are best compared to floppies and removable hard disk media given their possibility of easy and problem-free disk exchange and a capacity on the order of that of removable magnetic media (Tape, Bernoulli, SyQuest).

Generally, magnetic media and optical media do not compete; they complement each other due to their specific advantages. It can be expected that also in the future both system families will not stand in opposition to each other, but will and have to solve the upcoming problems of data storage together according to their specific characters and advantages.

The acceptance of optical data storage into the mass storage market, which is as yet exclusively dominated by magnetic systems, will be fundamentally boosted if optical drives and media are subject to uniform standards and become fully compatible, and multiuser drives are offered which enable the user to employ alternatively CD-ROM and EOD disks, and maybe WORM disks as well (and CD-R disks, respectively). A prerequisite, however, will be whether rewritable optical memories will use the MOR or the PCR process. This accord especially will be hard to reach.

Generally it can be said that optical systems will assume an ever increasing market share (depending on the achievement of uniform standards) of the data storage market which is currently dominated by magnetic systems. Additionally they will advance into new applications. Up to the end of the twentieth century, complementary technologies rather than a conflict between optical and magnetic mass memories are likely.

BIBLIOGRAPHY

Cited Publications

1. G. Kaempf, H. Loewer, and M. W. Witman, *Polym. Eng. Sci.* **27**, 1421 (1987); G. Kaempf, *Ber. Bunsenges. Phys. Chem.* **89**, 1179 (1985).
2. M. Hartmann, J. Braat, and B. Jacobs, *IEEE Trans. Magn.* **MAG-20**, 2013 (1984).
3. M. Emmelius, G. Pawlowski, and H. W. Vollmann, *Angew. Chem.* **101**, 1475 (1989).
4. K. Y. Law, P. S. Vincett, and G. E. Johnson, *Appl. Phys. Lett.* **39**, 718 (1981); D. G. Howe and J. J. Wrobel, *J. Vac. Sci. Technol.* **18**, 92 (1981).
5. V. Novotny and L. Alexandru, *J. Appl. Phys.* **50**, 1215 (1979), and *J. Appl. Polymer Sci.* **24**, 1321 (1979).
6. M. C. Gupta, *Appl. Opt.* **23**, 3950 (1984).
7. P. Kivits, R. De Bont, and P. Zalm, *Appl. Phys.* **24**, 273 (1981); P. Kivits and co-workers, *Thin Solid Films* **87**, 215 (1982); J. E. Kuder, *J. Imaging Technol.* **12**, 140 (1986).
8. M. Matsuoka, *Mol. Cryst. Liq. Cryst. Sci. Technol., Sect. A* **224**, 85 (1993); A. Kakuta, in M. Matsuoka, ed., *Infrared Absorbing Dyes*, Plenum Press, New York, 1990, H. T. Macholdt, *Chem. Unserev teit* **24**(4), 176 (1990); P. F. Foudon, in D. R. Waring, ed., *Chemical Applied Dyes*, Plenum Press, New York, 1990, p. 381; F. Jones, *Rev. Prog. Colov. Relat. Top.* **19**, 20 (1989).
9. V. P. Jipson and C. R. Jones, *J. Vac. Sci. Technol.* **18**, 105 (1981), and *IBM Techn. Discl. Bull.* **24**(1A), 298 (1981).

10. G. Kaempf, H. Loewer, and M. Witman, *Kunstst./German Plastics* **76**, 1077 (1986); M. Witman, L. Loewer, and G. Kaempf, *SPI/SPE Plastics-West*, 40 (1987).
11. D. J. Gravesteijn and J. van der Veen, *Philips Techn. Rev.* **41**, 325 (1983–1984); D. J. Gravesteijn, C. Steenbergen, and J. van der Veen, *Proc. SPIE Int. Soc. Opt. Eng.* **420**, 327 (1983).
12. R. S. Jones and J. E. Kuder, in K. L. Mittal, ed., *Proc. Amer. Chem. Soc. Symp. on Polymers in Information Storage Technology*, Los Angeles, Calif., Sept. 25–30, 1988, Plenum Press, New York, 1989, p. 3.
13. Eur. Pat. A 254,553 (1988), S. Hayashida and S. Tai (to Hitachi Chem. Co., Ltd.), Eur. Pat. A 279,426 (1986), R. S. Jones, D. E. Nikles, and M. E. Kenney (to Celanese Corp.), Eur. Pat. A 296,876 (1988), T. Seiji and co-workers, (to Hitachi Chem. Co., Ltd.).
14. T. Kanno, H. Watanabe, and S. Nozaki, *Proc. 34th Conf. Soc. Appl. Phys.*, 720 (1987); Jpn. Pat. 62–223, 287 (1987), K. Morikawa, H. Shibano, and H. Yamazaki, (to Kao Corp.); Jpn. Pat. 63–57, 287 (1988), S. Hirose and co-workers, (to Mitsui Toatsu Chem. Inc.).
15. Ger. Pat. A 3,711,762 (1988) B. Albert, H. Kuppelmaier, and G. Wagenblast (to BASF AG).
16. M. Ito and co-workers, *Proc. SPIE Int. Soc. Opt. Eng.* **420**, 332 (1983); K. Takagi and co-workers, *Dyes Pigm.* **6**, 177 (1985); S. H. Kim and co-workers, *Chem. Express* **2**, 73 (1987); S. H. Kim, M. Matsuoka, and T. Kitao, *Chem. Lett.*, 1351 (1985).
17. H. W. Vollmann, *J. Inf. Rec. Mater.* **20**, 3 (1992).
18. P. Kullik, ed., *Optische Speicherplattensysteme*, Teil 1, Arbeitsgemeinschaft für wirtschaftliche Verwaltung e.V., Schrift 448, 1988.
19. B. G. Huth, *IBM J. Res. Develop.* **18**, 100 (1974).
20. P. Hansen, *J. Appl. Phys.* **63**, 2364 (1988).
21. M. Mansuripur, *J. Appl. Phys.* **66**, 6175 (1989).
22. S. Klahn and D. Raasch, *IEEE Trans. Magn.* **MAG-26**, 1918 (1990); R. A. Hajjar and H-P. D. Shieh, *J. Appl. Phys.* **68**, 4199 (1990).
23. S. Tsunashima, H. Tsuji, and S. Uchiyama, *J. Magn. Soc. Jpn.* **5**, 973 (1981).
24. C. J. Lin, *J. Appl. Phys*, **67**, 4409 (1990).
25. S. Ohnuki and co-workers, *Moris 91*, 18-K-03 (1991); *J. Magn. Soc. Jpn.* **15**, (S1), 399 (1991).
26. N. Ohta and co-workers, *SPIE* **1663**, 232 (1992).
27. H. Kronmüller, *Phys. Stat. Sol.* **144**(b), 385 (1987).
28. R. J. Gambino, P. Chaudhaari, and J. J. Cuomo, *AIP Conf. Proc.* **18**, 578 (1974).
29. J. Orehotsky and K. Schröder, *J. Appl. Phys.* **43**, 2413 (1972).
30. P. Chaudhari, J. J. Cuomo, and R. J. Gambino, *Appl. Phys. Lett.* **22**, 337 (1973).
31. P. Hansen, in K. H. J. Buschow, ed., *Handbook of Magnetic Materials*, Vol. **6**, Elsevier Science Publishers B.V., New York, 1991, Chapt. 4.
32. X. Hu and co-workers, *Proc. Intermag '93*, Stockholm, 1993.
33. P. Hansen and H. Heitmann, *IEEE Trans. Magn.* **25**, 4390 (1989).
34. C. J. Lin, *Mat. Res. Soc. Symp. Proc.* **150**, 15 (1989).
35. F. J. A. M. Greidanus and W. B. Zeper, *MRS Bulletin* **15**(4), 31 (1990).
36. D. Mergel, P. Hansen, and S. Klahn, *Mat. Sci. Forum* **62–64**, pt II, 547 (1990).
37. M. Hartmann and co-workers, *J. Mag. Soc. Jpn.* **15**(S1), 165 (1991).
38. D. Mergel and co-workers, *NATO ASI Series B* **259**, 249 (1991).
39. D. Mergel, P. Hansen, and D. Raasch, *Proc. SPIE 1663, Optical Data Storage 1992*, 240 (1992).
40. D. J. Sellmyer, R. D. Kirby, and S. S. Jaswal, "The Magnetism of Amorphous Metals and Alloys", in J. A. Fernandez-Baca and W. Y. Ching, eds., World Scientific Publishing, Ltd., 1993.
41. P. Hansen and co-workers, *J. Appl. Phys.* **66**, 756 (1989).
42. P. Hansen and co-workers, *J. Appl. Phys.* **69**, 3194 (1991).
43. D. H. Ryan and co-workers, *Phys. Rev. B* **40**, 11208 (1989).
44. T. Suzuki, C. J. Lin, and A. E. Bell, *IEEE Trans. Magn.* **MAG-24**, 2452 (1988).
45. D. Mergel, H. Heitmann, and P. Hansen, *Phys. Rev. B* **47**, 882 (1993).
46. V. G. Harris and co-workers, *Phys. Rev. Lett.* **69**, 1939 (1992).
47. F. Hellman and E. M. Gyorgy, *Phys. Rev. Lett.* **68**, 1391 (1992).
48. R. Sato, N. Saito, and Y. Togami, *Jpn. J. Appl. Phys.* **24**, 1266 (1985).

49. Y. Aoki and co-workers, *IEEE Trans. Magn.* **MAG-21**, 1624 (1985).
50. C. J. Lin and A. E. Bell, *Fourth Joint MMM/Intermag Conf.*, Vancouver, AE-02, 1988.
51. D. Raasch, *J. Magn. Soc. Jpn.* **17** (S1), 192 (1993).
52. P. F. Carcia and D. Meinhalt, *Appl. Phys. Lett.* **47**, 178 (1985).
53. S. Hashimoto, Y. Ochiai, and K. Aso, *J. Appl. Phys.* **66**, 4909 (1989).
54. S. Hashimoto and Y. Ochiai, *J. Mag. Magn. Mat.* **88**, 211 (1990).
55. F. J. A. M. Greidanus and co-workers, *Appl. Phys. Lett.* **54**, 2481 (1989).
56. J. Ferre and co-workers, *Appl. Phys. Lett.* **56**, 1588 (1990).
57. W. P. Zeper and co-workers, *J. Appl. Phys.* **65**, 4971 (1989).
58. W. P. Zeper, F. J. A. M. Greidanus, and P. F. Carcia, *IEEE Trans. Magn.* **MAG-25**, 3764 (1989).
59. D. Weller and W. Reim, *Mat. Res. Soc. Symp. Proc.* **232**, 71 (1991).
60. P. F. Carcia, S. I. Shah, and W. B. Zeper, *Appl. Phys. Lett.* **56**, 2345 (1990).
61. P. F. Carcia and co-workers, *Appl. Phys. Lett.* **58**, 191 (1991).
62. H. W. Van Kesteren and W. B. Zeper, *JMMM* **120**, 271 (1992).
63. D. Raasch, *IEEE Trans. Magn.* **29**, 34 (1993).
64. S. Sumi and co-workers, *J. Magn. Soc. Jpn.* **15**(S1), 365 (1991).
65. S. Hashimoto and co-workers, *JMMM* **121**, 471 (1993).
66. W. P. Zeper and co-workers, *IEEE Trans. Magn.* **28**, 2503 (1992).
67. S. Hashimoto, A. Maesaka, and Y. Ochiai, *J. Appl. Phys.* **70**, 5133 (1991).
68. D. Mergel and co-workers, *SPIE* **1274**, 270 (1990).
69. P. Hansen, J. P. Krumme, and D. Mergel, *J. Magn. Soc. Jpn.* **15**(S1), 219 (1991).
70. J. W. D. Martens and A. B. Voermans, *IEEE Trans. Magn.* **MAG-20**, 1007 (1984).
71. M. Gomi, K. Utsugi, and M. Abe, *IEEE Trans. Magn.* **MAG-22**, 1233 (1986); J. P. Krumme and co-workers, *J. Appl. Phys.* **66**, 4393 (1989).
72. A. Hoh, *Jpn. J. Appl. Phys.* **28**(53), 15 (1989).
73. Y. Kaneko and Y. Sawada, *Jpn. J. Appl. Phys.* **26**(S), 23 (1987).
74. Ger. Pat. 3,716,392, Y. Kaneko and F. Ohmi.
75. K. Shono and co-workers, *MRS Sympos. F 3-2*, Materials Research Society, Pittsburgh, Pa., 1989.
76. S. Tsunashima and co-workers, *IEEE Trans. Mag.* **MAG-17**, 2840 (1981).
77. R. J. Gambino, T. S. Plaskett, and R. R. Ruf, *IEEE Trans. Magn.* **24**, 2557 (1988).
78. H. Iiyori and S. Takayama, *J. Appl. Phys.* **69**, 4761 (1991).
79. J. Saito and co-workers, *Jpn. J. Appl. Phys.* **26**(S4), 155 (1987).
80. A. Okamuro and co-workers, *J. Magn. Soc. Jpn.* **15**(S1), 447 (1991).
81. K. Aratani and co-workers, *SPIE* **1499**(ODS) 209 (1991).
82. A. Fukumoto and co-workers, *SPIE* **1499** (Optical Data Storage), 216 (1991).
83. H. Iida and co-workers, *ISOM'89* **28**, B-20 (1989); *JJAP.* **28**, 367 (1989).
84. T. Tokunaga, *J. Appl. Phys.* **67**, 4417 (1990).
85. D. Raasch, *J. Mag. Magn. Mat.* **101**, 202 (1991).
86. K. Aratani and co-workers, *Proc. SPIE* **1078**(ODS), 258 (1989).
87. Y. Muto and co-workers, *J. Magn. Soc. Jpn.* **15**(S1), 311 (1991).
88. S. Tanaka and co-workers, *J. Magn. Soc. Jpn.* **15**(S1), 331 (1991).
89. K. Hayashi and O. Okada, *J. Magn. Soc. Jpn.* **15**(S1), 335 (1991).
90. M. Miyamoto and co-workers, *J. Magn. Soc. Jpn.* **15**(S1), 339 (1991).
91. T. K. Hatwar and D. G. Stinson, *J. Appl. Phys.* **69**, 6439 (1991).
92. A. Nakaoki and co-workers, *J. Magn. Soc. Jpn.* **17**(S1), 363 (1993).
93. T. Tokimaga and co-workers, *J. Magn. Soc. Jpn.* **17**(S1), 357 (1993).
94. T. Fukami and co-workers, *J. Appl. Phys.* **67**, 4415 (1990).
95. K. Tsutsumi, *J. Mag. Magn. Mat.* **120**, 247 (1993).
96. D. Mengel, *J. Appl. Phys.* **69**, 4520 (1991).
97. D. Mengel, *J. Appl. Phys.* **70**, 6433 (1991).
98. T. Kobayashi and co-workers, *JJAP.* **20**, 2089 (1981).
99. D. Mergel, *J. Appl. Phys.* **74**, 4072 (1993).

100. T. Fukami and co-workers, *J. Magn. Soc. Jpn.* **15**(S1), 293 (1991).
101. H. W. Vollmann, *Chem. Ind.*, 68 (Oct. 1989).
102. J. W. M. Biesterbos and co-workers, *Thin Solid Films* **58**, 259 (1979); R. Hasegawa and R. C. Taylor, *J. Appl. Phys.* **46**, 3606 (1975); R. B. van Dover, *J. Appl. Phys.* **59**, 1291 (1986).
103. M. Libera and M. Chen, *MRS Bulletin* **15**(4), 40 (1990).
104. E. M. Engler, *Adv. Mater.* **2**, 166 (1990).
105. A. E. Bell, in M. J. Weber, ed., *Handbook of Laser Science and Technology*, Vol. **5**, Part 3, CRC Press, Boca Raton, Fla., 1987, p. 65.
106. M. Takenaga and co-workers, *Proc. Photo-Opt. Inst. Eng.* **420**, 173 (1983).
107. A. W. Smith, *Appl. Opt.* **13**, 795 (1974).
108. B. Ryan, *BYTE*, 289 (Nov. 1990).
109. K. A. Rubin, *J. Magn. Soc. Jpn.* **16**(S1), 127 (1991).
110. K. Nishimura and co-workers, *Jpn. J. Appl. Phys.* **28**(3), 135 (1989).
111. K. A. Rubin, *Mat. Res. Soc. Symp. Proc.* **230**, 239 (1992).
112. M. Chen and A. Rubin, *Proc. Soc. Photo Opt. Instrum. Eng.* **1078**, 150 (1989); M. Chen and co-workers, *Appl. Phys. Lett.* **46**, 734 (1985).
113. H. Yamazaki and co-workers, *Adv. Mater.* **5**, 214 (1993).
114. D. P. Birnie, in D. R. Uhlmann and D. R. Ulrich, eds., *Ultrastructure Processing of Advanced Materials*, John Wiley & Sons, Inc., New York, 1992, p. 475.
115. S. R. Ovshinsky, *J. Non-Cryst. Solids* **141**, 200 (1992).
116. T. Ohta and co-workers, *Jpn. J. Appl. Phys.* **28**(3), 123 (1989); H. Ishibashi, M. Moriya, and T. Ohta, *SPIE* **1663** (Optical Data Storage), 427 (1992).
117. I. Morimoto and co-workers, *SPIE* **1663** (Optical Data Storage), 294 (1992).
118. D. E. Nikles and co-workers, *Proc. Soc. Photo Opt. Instrum. Eng.* **1078**, 43 (1989); P. K. Chan and T. R. Hart, *Appl. Opt.* **28**, 1685 (1989); S. Y. Suh and co-workers, *Proc. Soc. Photo Opt. Instrum. Eng.* **1078**, 189 (1989); H. A. Goldberg and co-workers, *Proc. Soc. Photo Instrum. Eng.* **1078**, 170 (1989).
119. M. C. Gupta, *J. Appl. Phys.* **60**, 2932 (1986).
120. N. E. Iwamoto and J. M. Halter, in Ref. 11, p. 117; W. E. Skiens and G. A. Russell in Ref. 12, p. 133; J. M. Halter and N. Iwamoto, *Proc. Soc. Photo Instrum. Eng.* **899**, 201 (1988); M. A. Lind and J. S. Hartman, *Proc. Soc. Photo Instrum. Eng.* **899**, 211 (1988); J. S. Hartman and co-workers, *Proc. Soc. Photo Instrum. Eng.* **1078**, 80 (1989).
121. G. Kaempf, *Polymer J.* **19**, 257 (1987).
122. *High Tech. Materials Alert*, 2 (Jan. 1985).
123. J. E. Kuder, *J. Imaging Technol.* **12**, 140 (1986); F. E. Luborsky, *Mater. Res. Soc. Symp. Proc.* **80**, 375 (1987); R. P. Freeze, *IEEE Spectrum* **25**, 41 (1988); D. A. Carlin, Y. Tsunoda, and A. A. Jamberdino, *Proc. SPIE Int. Soc. Opt. Eng.*, 899 (1988); G. R. Knight and C. N. Kurtz, eds., *Proc. SPIE Int. Soc. Opt. Eng.*, **1078** (1989).
124. H. Dürr, *Angew. Chem.* **101**, 427 (1989).
125. H. Menzel, *Nachr. Chem. Tech. Lab.* **39**, 636 (1991).
126. R. Bertelson, in G. H. Brown, ed., *Techniques of Chemistry*, Vol. **3**, Wiley-Interscience, New York, 1971; N. S. Allen and J. F. McKellar, eds., *Photochemistry of Dyed and Pigmented Polymers*, Applied Science Publishers, London, 1989.
127. M. Kryszewski and P. Uznanski, *Proc. Int. Symp. PME'89, Tokyo 1989*, Kodansha Publ. Tokyo, 1990, and VCH, Weinheim, 1990, p. 549; M. Gehrtz, C. Bräuchle, and J. Voitländer, *J. Amer. Chem. Soc.* **104**, 2094 (1982); C. Lenoble and R. S. Becker, *J. Phys. Chem.* **90**, 62 (1986).
128. Z. G. Garlund, *J. Polym. Sci. Polym. Lett. Ed.* **6**, 57 (1968).
129. M. Kryzsewski, D. Lapiensis, and B. Nadolski, *J. Polym. Sci. Polym. Chem. Ed.* **11**, 2423 (1973); M. Kryszewski and co-workers, *J. Chem. Soc. Faraday Trans. II* **76**, 351 (1980).
130. Brit. Pat. 2,441,759 (Mar. 13, 1975), H. G. Heller, H. G. Heller, *Chem. Ind. London*, (**6**), 193 (1978); H. G. Heller, *IEEE Proc.* **130**, 209 (1983); A. P. Glaze and co-workers, *J. Chem. Soc. Perkin Trans.*, 957 (1985).
131. R. J. Hart and H. G. Heller, *J. Chem. Soc. Perkin Trans.*, 1321 (1972); G. A. Delzenne, *Adv. Photochem.* **11**, 2 (1979); H. G. Heller and co-workers, *J. Chen. Soc. Perkin Trans.*, 1487 (1974), *Ibid.*, 571 (1978), *Ibid.*, 202 (1981), *Ibid.*, 315 (1986); *Ibid.*, 1599 (1986); F. Eplattenier, *Swiss Chem.* **7**, 19 (1985).
132. I. Cabrera, V. Krongauz, and H. Ringsdorf, *Angew. Chem.* **99**, 1204 (1987), and *Angew. Chem. Int. Ed. Engl.* **26**, 1178 (1987); Y. Suzuki and co-workers, *Polym Bull.* **17**, 285 (1987).

133. J. F. Cameron and J. M. J. Frechet, *Macromolecules* **24**, 1088 (1991).
134. H.-W. Schmidt, *Angew. Chem. Adv. Mater.* **101**, 964 (1989).
135. M. Eich and H. J. Wendorff, *Makromol. Chem. Rapid Commun.* **8**, 467 (1987); M. Eich and co-workers, *Proc. SPIE Int. Soc. Opt. Eng.* **682**, 93 (1987).
136. I. Cabrera, A. Dittrich, and H. Ringsdorf, *Angew. Chem.* **103**, 106 (1991).
137. V. P. Shibaev and co-workers, *Polym. Comm.* **24**, 364 (1983); V. P. Shibaev and N. A. Plate, in *Advances in Polymer Science, 60/61*, 173, Springer-Verlag, Berlin, 1984.
138. H. J. Coles and R. Simon, *Polymer* **26**, 1801 (1985); H. J. Coles, *Faraday Discuss. Chem. Soc.* **79**, 201 (1985); M. Eich and co-workers, *Makromol. Chem. Rapid Commun.* **8**, 59 (1987).
139. T. Ikeda and co-workers, *Chem. Lett.*, 1679 (1988); T. Ikeda and co-workers, *Mol. Cryst. Liq. Cryst.* **182 B**, 357 and 373 (1990); T. Ikeda and co-workers, *Ibid.* **188**, 207 and 223 (1990); T. Ikeda and co-workers, *Mol. Cryst. Liq. Cryst.* **188**, 235 (1990).
140. T. Ikeda and co-workers, *Macromolecules* **23**, 42 (1990).
141. M. Eich and J. H. Wendorff, *Mol. Cryst. Liq. Cryst.* **169**, 133 (1989); R. Birenheide and H. J. Wendorff, *SPIE Proc.*, 1213 (1990); K. Anderle, R. Birenheide, and H. J. Wendorff, *BMFT-Workshop* (*Ue???336???uc Werkstoffe*), Dresden, 1991, Congress Book, p. 507, and Makromol. Chem. Macromol. Sympos., (1991), Congress Book, p. 44; K. Anderle and co-workers, *Makromol. Chem. Rapid Comm.* **10**, 477 (1989).
142. J. Stumpe and co-workers, *J. Inf. Rec. Mat.* **27**, 449 (1994); J. Stumpe and co-workers, *Makromol. Chem. Rapid Commum.* **12**, 81 (1991); Th.Fischev and co-workers, *J. Photochem. Photobiol. A: Chem.* **80**, 453 (1994); L. Laeskev and co-workers, *Mol. Cryst. Liq. Cryst.* **246**, 347 (1994).
143. J. Pinsl, C. Bräuchle, and F. H. Kreuzer, *J. Mol. Electr.* **3**, 9 (1987).
144. S. Hvilsted, F. Andruzzi, and P. S. Ramanujam, *Opt. Lett.* **17**, 1234 (1992).
145. K. Anderle and H. J. Wendorff, *Mol. Cryst. Liq. Cryst.*, 191 (1993), in press.
146. G. Wagenblast, K. Beck, and K.-H. Etzbach, *205th Nat. Meeting ACS*, Denver, Colo., 1993, preprints p. 699, and *Nat. Meeting ACS*, Chicago, Ill. (1993), preprints **34**, 709 (1993); Ger. Pat. 3,704,146 (1988), G. Wagenblast, K.-H. Etzbach, and B. Hisgen (to BASF AG).
147. K. Ichimura and co-workers, *Makromol. Chem. Rapid Commun.* **10**, 5 (1989); S. Tazuke, *Kokagaku* **12**, 85 (1988).
148. W. Hickel and co-workers, *Makromol. Chem. Rapid Commun.* **10**, 353 (1989); M. Sawodny and co-workers, *Makromol. Chem., Macromol. Symp.* **46**, 217 (1991).
149. K. Ichimura and co-workers, *Langmuir* **4**, 1214 (1988).
150. T. Seki and co-workers, *Macromolecules* **22**, 2305 (1989).
151. U. Wiesner and co-workers, *Makromol. Chem.* **191**, 2133 (1990).
152. T. Seki and co-workers, *2nd Int. Sympos. on Chemistry of Functional Dyes*, Osaka, Japan, 1992, Paper P-042, *Congress Book*, p. 91.
153. U. Wiesner and co-workers, *Liq. Cryst.* **11**, 251 (1992).
154. K. Ichimura and M. Sakuragi, *J. Polym. Sci. Lett. Ed.* **26**, 185 (1988); A. Tshuchida, M. Nakano, and M. Yamamoto, *Proc. Int. Symp. PME'89*, Tokyo 1989, Kodansha Publ., Tokyo, 1990 and VCH, Weinheim, 1990, p. 541; C. Bräuchle and co-workers, *Optics Lett.* **6**, 159 (1981); *Ibid.* **7**, 177 (1982).
155. M. Sisido and co-workers, *Macromolecules* **24**, 3993 (1991).
156. N. Hampp, C. Bräuchle, and D. Oesterhelt, *J. Biophys.* **58**, 83 (1986); N. Hampp and C. Brüuchle, in H. Dürr and H. Bouas-Laurent, eds., *Photochromism*, Elsevier, Amsterdam, 1990, p. 954.
157. R. R. Birge, *Annu. Rev. Phys. Chem.* **41**, 683 (1990).
158. D. Oesterhelt, C. Bräuchle, and N. Hampp, *Quarterly Rev. of Biophys.* **24**(4), 425 (1991).
159. R. Margalit and J. Yu, *IEEE EMBS* **12**, 1717 (1990); C. Bräuchle, N. Hampp, and D. Oesterhelt, *Adv. Mater.* **3**(9), 420 (1991); C. Bräuchle and N. Hampp, *BPS'91*, Bayreuth, Germany, 1991, *Congress Book*, p. 102.
160. N. Hampp, C. Bräuchle, and D. Oesterhelt, *4th Int. Sympos. on Bioelectronic and Electronic Devices*, Miyazaki, Japan, 1992, Congress Book, p. 72; N. Hampp, D. Oesterhelt, and C. Bräuchle, *Proc. Holographics'90*, Nürnberg, Germany, Congress Book, p. 65; N. Hampp, C. Bräuchle, and D. Oesterhelt, *MSR-Bulletin*, p. 56, Nov. 1992.
161. W. Lahti and D. McCarron, *BYTE* **15**, 311 (1990).
162. General Presentation, Laser Card (Optical Memory Card), Drexler Technology Corp., 1989.
163. G. Kaempf, D. Freitag, and W. Witt, *Angew. Makromol. Chem.* **183**, 243 (1990).
164. L. DÀuria, J. P. Huignard, C. Slezak, and E. Spitz, *Appl. Opt.* **13**, 808 (1974).

165. J. H. Strickler and W. W. Webb, *Adv. Mater.* **5**, 479 (1993).
166. W. K. Swainson and S. D. Kramer, U.S. Patents 4,471,470 and 4,466,080 (1984).
167. S. Esener and P. M. Rentzepis, *Proc. SPIE-Int. Soc. Opt. Eng.* **1499**, 144 (1991).
168. W. Denk, J. H. Strickler, and W. W. Webb, *Science* **248**, 73 (1990).
169. E. Krätzig and co-workers, *Proc. SPIE Int. Soc. Eng.* **164**, 33 (1979); H. Franke, H. G. Festl, and E. Krätzig, *Colloid Polym. Sci.* **262**, 213 (1984); M. Kopietz and co-workers, *Polym. Photochem.* **5**, 109 (1984); M. Kopietz, M. D. Lechner, and D. G. Steinmeier, *Eur. Polym. J.* **20**, 667 (1984).
170. *Chem. Rundschau*, (14) p. 5, (Apr. 1985).
171. M. D. Lechner and co-workers, Makromol. Kolloq., Freiburg, Germany, 1985, Congress Book, p. 78; T. Parish, *BYTE* **15**, 283 (1990).
172. M. Irie and K. Sayo, *J. Phys. Chem.* **96**, 7671 (1992).
173. U.S. Pat. 4,101,976 (1978), G. Castro and co-workers; J. Friedrich and D. Haarer, *Angew. Chem.* **96**, 96 (1984), and *Angew. Chem. Int. Ed. Engl.* **23**, 113 (1984); W. E. Moerner, T. P. Carter, and C. Bräuchle, *Appl. Phys. Lett.* **50**(8), 430 (1987); W. E. Moerner, ed., *Persistent Spectral Hole-Burning*, Science and Applications, Springer, Berlin, 1988; W. E. Moerner, *Jpn. J. Appl. Phys.* **28**, 221 (1989).
174. U. P. Wild, S. E. Bucher, and F. A. Burkhalter, *Appl. Opt.* **24**, 1526 (1985); A. Renn and U. P. Wild, *Appl. Opt.* **26**, 4040 (1987); U. P. Wild and co-workers, *Jpn. J. Appl. Phys.* **26**, 233 (1987); U. P. Wild and A. Renn, *Proc. SPIE Int. Soc. Opt. Eng.* **910**, 61 (1988); Y. Jino and co-workers, *Chem. Phys. Lett.* **140**, 76 (1987).
175. U. P. Wild and co-workers, *Proc. Int. Symp. PME'89*, Tokyo 1989, Kodansha Publ., Tokyo, 1990 and VCH, Weinheim, 1990, p. 507; U. P. Wild, A. Rebane, and A. Renn, *Adv. Mater.* **3**(3), 453 (1981).
176. K. Ao, S. Jahn, L. Kuemmerl, K. Weiner, and D. Haarer, *Jpn. J. Appl. Phys.* **31**, 693 (1992).
177. T. P. Carter and co-workers, *J. Phys. Chem.* **91**, 3998 (1987).
178. H. Suzuki and T. Shimada, *Mol. Cryst. Liq. Cryst.* **217**, 165 (1992) and *Jpn. J. Appl. Phys.* **31**, 706 (1992); H. Suzuki and co-workers, *J. Lumin.* **53**, 271 (1992).
179. H. Suzuki, T. Shimada, and H. Hiratsuka, *Chem. Phys. Lett.* **183**, 570 (1991).
180. G. Fuxi, *Proc. SPIE-Int. Soc. Opt. Eng.* **1519**, 530 (1991); D. Wang and co-workers, *Chinese Phys. Letts.* **12**, 556 (1990).
181. H. Suzuki, *Adv. Mater.* **5**, 216 (1993).
182. J. Hennig, *Kunststoffe* **75**, 425 (1985); J. Hennig, *Angew. Makromol. Chem.* **145/146**, 391 (1986).
183. S. Anders and B. Hardt, *Kunststoffe* **77**, 21 (1987); S. Anders, H. Schmid, and K. Sommer, *Kunststoffe* **79**, 55 (1989).
184. U.S. Pat. 2,938,232 (1960), F. A. Martin (to Hoover Co.); U.S. Pat. 2,443,286 (1948), Johnson; U.S. Pat. 4,008,031 (1975), H. P. Weber; U.S. Pat. 4,828,769 (1989), S. M. Maus and G. J. Galic.
185. A. Iwasawa and N. Funakoshi, in Ref. 11, p. 207; M. Takeshima and N. Funakoshi, *Proc. SID* **25**(3), 219 (1984).
186. G. Kaempf, *J. Inf. Record. Mater.* **18**, 83 (1990).
187. R. M. Pisipati, H. Schmid, and G. Kaempf, *MRS Bulletin* **15**(4), 46 (1990).
188. W. Siebourg and co-workers, *Polym. Eng. Sci.* **30**, 1133 (1990).
189. J. Hennig, *Proc. Int. Symp. on Optical Memory* (1987); *Jpn. J. Appl. Phys.* **26**(4), 9 (1987).
190. G. Kaempf and co-workers, *Proc. Int. Symp. PME'89*, Tokyo, 1989, Kodansha Publ., Tokyo, 1990, and VCH, Weinheim, 1990, p. 549.
191. W. Siebourg, *Kunststoffe* **76**, 917 (1986).
192. D. Freitag, G. Fengler, and L. Morbitzer, *Angew. Chem.* **103**, 917 (1991).
193. Product Information "Makrolon CD-2005", No. 155, 4/89, 5M (1989), Mobay Corp., Pittsburgh, Pa., Anwendungstechn, Inform. ATI 735 (1989), Bayer AG Leverkusen, Germany.
194. H. Guyot, *Plast. Europe*, 289 (July 1992).
195. G. Kaempf, D. Freitag, and G. Fengler, *Kunststoffe* **82**, 385 (1992), and *Kunstst. German Plastics* **82**, 9 (1992).
196. G. Kaempf and co-workers, *J. Polym. Adv. Technol.* **3**, 169 (1992).
197. G. H. W. Buning and co-workers, *Proc. Int. Symp. on Optical Memory ISOM'87*, Poster WC 23.
198. G. Kaempf and co-workers, *Polym. Prepr., Amer. Chem. Soc., Div. Polym. Chem.* **29**, 209 (1989).
199. Eur. Pat. 249,963 (1987) and Jpn. Pat. 023,658 (1989), K. Shigematsu, T. Nakagawa, and S. Shuji (to Idemitsu-Kosan Co. Ltd.); Ger. Pat. 3,835,203 (1990), K. Berg and co-workers (to Bayer AG Leverkusen).
200. Jpn. Pat. 1,087,621 (1987), I. Takahashi and T. Sugano (to Daicel Chem. Ind.).
201. D. Freitag and co-workers, in J.I. Kroschwitz, ed., *Encyclopedia of Polymer Science and Engineering*, Vol. **11**, John Wiley & Sons, Inc., New York, 1988, p. 648.

202. Jpn. Pat. 242,474 (1989), (to Daicel Chem. Ind.). Eur. Par. 249,963 (1987), K. Shigematsu, T. Nakagawa, and S. Shuji (to Idemitsu-Kosan Co. Ltd.).
203. K. C. Stueben, *J. Polym. Sci.* **A3**, 2309 (1965); Eur. Pat. 287,887 (1988), L. R. Faler and J. C. Lynch (to General Electric Co.).
204. D. Freitag and U. Westeppe, *Makromol. Chem. Rapid Commun.* **12**, 95 (1991); Ger. Pat. 3,832,396 (1990), D. Freitag and co-workers (to Bayer AG).
205. G. Kaempf, *Kunststoffe* **82**, 1097 (1992).
206. *Apec-HT Application Technology Information*, ATI 849e, Mobay Corp., Pittsburgh, Pa., 1992; *Anwendungstechn. Information*, ATI 489, Bayer AG, Leverkusen, Germany, 1992.
207. N. Isobe and S. Imai, *Sumitomo Chem. Co. Ltd.*, Chem. Research Lab, 1986.
208. Jpn. Pat 3,196,612 (1988), (to Mitsubishi Gas Chem. Ltd.); Jpn. Pat. 3,199,735 (1987), M. Okamoto and S. Nishiyama (to Idemitsu Kosan Petrochem. Co. Ltd.).
209. V. Serini, D. Freitag, and H. Vernaleken, *Angew. Makromol. Chem.* **55**, 175 (1976); Ger. Pat. 3,807,098 (1988) and Ger. Pat. 3,823,196 (1990) V. Serini and co-workers, (to Bayer AG).
210. G. H. W. Buning and R. M. R. Gijsen, *Polym. Prepr. Amer. Chem. Soc. Div. Polym. Chem.* **29**, 211 (1988).
211. Nippon Chemtec. Consult Inc., Research and Development Review Report No. 34, Apr. 1986.
212. H. Jaeger, E. J. Vorenkamp, and G. Challa, *Polym. Comm.* **24**, 290 (1983).
213. B. R. Hahn and J. H. Wendorff, *Polymer* **26**, 1619 (1985).
214. A. Todo and H. Kajiura, *Purasuchikkura (Japan Plastics)* **38**, 41 (1987).
215. V. Dragutan, A. T. Balaban, and M. Dimonie, *Olefin Metathesis and Ring-Opening Polymerization of Cyclo-Olefins*, 2nd ed., Wiley-Interscience, New York, 1985, *J. C. Mol, J. Mol. Catal.* **65**, 145 (1991).
216. W. Interthal, lecture, *Polymere in der optischen Informationsverarbeitung*, Frühjahrstagung FA Polymerphysik der DPG, Bayreuth, Germany, 1992.
217. *Mod. Plastics Ind.*, 16 (July 1992).
218. *Hoechst High Chem Mag.* **14**, 48 (1993); *Nachr. Chem. Tech. Lab.* **41**, 724 (1993); *Mod. Plastics Int.*, 11 (July 1993).
219. T. Kohara, M. Ohshima, and T. Natsuume, *Mater. Res. Soc. Symp. Proc., Boston* 1989, paper Q 12.9.
220. Eur. Pat. 254,184 (1987), W. Kloeker and co-workers (to Bayer AG); U.S. Pat. 5,052,916 (1991), W. Kloeker and co-workers (to Bayer AG).
221. *Chem. Eng.* (Sept. 29, 1986); Jpn. Pat. 58-176,204 (1983), (to Mitsubishi Petrochem. Ind. Ltd.).
222. K. Manabe and co-workers, *Polym. Prepr., Amer. Chem. Soc. Div. Polym. Chem.* **29**, 230 (1988).
223. W. Interthal, Hoechst AG, and Frankfurt, private communication.
224. *Optical Memory News* **12**, 42 (1988).
225. H. Ohishi and co-workers, *Polym. Prepr.* **32**, 152 (1991).
226. T. H. Wallmann, M. C. A. Mathur, and M. H. Kryder in Ref. 12, p. 175.

GÜNTHER KÄMPF
University of Aachen
DIETER MERGEL
University of Essen

Related Articles

Information storage, magnetic; Holography; Photography